

Understanding Multimodal Complementarity for Single-Frame Action Anticipation

Manuel Benavent-Lledo, Konstantinos Bacharidis, Konstantinos Papoutsakis,
Antonis Argyros, and Jose Garcia-Rodriguez

Abstract—Human action anticipation is commonly treated as a video understanding problem, implicitly assuming that dense temporal information is required to reason about future actions. In this work, we challenge this assumption by investigating what can be achieved when action anticipation is constrained to a single visual observation. We ask a fundamental question: how much information about the future is already encoded in a single frame, and how can it be effectively exploited? Building on our prior work on Action Anticipation at a Glimpse (AAG), we conduct a systematic investigation of single-frame action anticipation enriched with complementary sources of information. We analyze the contribution of RGB appearance, depth-based geometric cues, and semantic representations of past actions, and investigate how different multimodal fusion strategies, keyframe selection policies and past-action history sources influence anticipation performance. Guided by these findings, we consolidate the most effective design choices into AAG+, a refined single-frame anticipation framework. Despite operating on a single frame, AAG+ consistently improves upon the original AAG and achieves performance comparable to, or exceeding, that of state-of-the-art video-based methods on challenging anticipation benchmarks including IKEA-ASM, Meccano and Assembly101. Our results offer new insights into the limits and potential of single-frame action anticipation, and clarify when dense temporal modeling is necessary and when a carefully selected glimpse is sufficient.

Index Terms—Action anticipation, multimodal, transformer, vision-language model, single-frame

I. INTRODUCTION

HUMAN action anticipation aims to predict an upcoming action before it occurs. This capability is fundamental to proactive perception systems, enabling early, safe and effective planning in a wide range of real world scenarios such as autonomous driving [1]–[3], procedural industrial tasks [4], [5] or human-robot collaboration [6]–[8]. Rather than acting reactively, anticipation allows systems to prepare for what is about to happen and adjust their behavior accordingly. In structured procedural tasks such as industrial assembly and maintenance, action anticipation is particularly valuable. Anticipating the next step enables downstream decision making,

M. Benavent-Lledo and J. Garcia-Rodriguez are with the Department of Computer Technology, University of Alicante, Carr. de San Vicente del Raspeig s/n, E-03690 San Vicent2 del Raspeig, Alicante, Spain
E-mail: {mbenavent,jgarcia}@dtic.ua.es

K. Bacharidis, K. Papoutsakis and A. Argyros are with the Institute of Computer Science, FORTH, Heraklion GR-700 13, Greece.
E-mail: {kbach,papouts,argyros}@ics.forth.gr

K. Bacharidis and A. Argyros are with the Computer Science Department, University of Crete, Heraklion, GR-700 13, Greece.

K. Papoutsakis is with the Department of Management, Science and Technology, Hellenic Mediterranean University, Heraklion, GR-714 10, Greece.

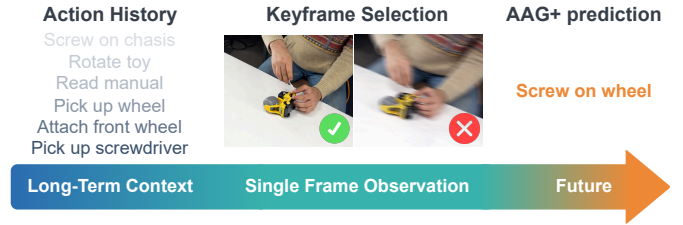


Fig. 1: **Do we need full video for action anticipation, or does a single frame suffice?** By fusing a semantic action history with an informative frame, our model matches in performance that of dense video-based approaches. In this work, we also study the roles of various modalities, fusion strategies, and choices of action history source and keyframe selection methods in overall performance.

reduces interruptions, and enables early detection of unsafe or erroneous transitions, supporting both productivity and safety.

Most contemporary anticipation methods approach the problem as dense video understanding [9]–[12], using short- and long-range temporal aggregation to infer intent from motion and evolving context. More recent approaches further incorporate multimodal cues (e.g., audio, pose, or object interactions) [13]–[19], increasing the amount of information processed per time step. While effective, these strategies often require processing vast amounts of temporally correlated data and learning temporal dynamics over extended horizons, increasing computational cost and modeling complexity. However, a key observation is that temporal redundancy is often high [20]–[24]. This property is particularly pronounced in procedural and instructional settings, where anticipation-relevant evidence often appears in brief moments that reveal object states, grasp configurations, and intermediate completion signals. Such observations can be interpreted as priors that reveal constrain or impose preconditions to plausible action transitions. This insight motivates us to seek for an alternative paradigm, that of *single-frame anticipation* (Fig. 1), in which anticipation is performed from a single observation augmented with contextual cues rather than from dense temporal encoding.

Single-frame anticipation is a challenging problem because without additional priors, a single image may reveal only partial task progress and intent. Consequently, the key question is not whether a single frame alone can match video-based modeling, but how to combine appearance with contextual priors to recover much of the benefit of temporal reasoning

that enables state-of-the-art performance, while reducing its modeling complexity. In our previous work [25], we introduced Action Anticipation at a Glimpse (AAG), a framework demonstrating that a single RGB frame, when augmented with additional modalities, can compete with video-based methods for action anticipation. Specifically, we showed that combining RGB appearance, geometric cues from depth, and semantic summaries of previously executed actions, enables accurate anticipation without relying on dense video processing. While these results were promising, they left several important questions unanswered regarding *how* and *why* such multimodal single-frame representations succeed.

In this work, we set out to extend this investigation and address these questions by systematically studying multimodal complementarity in the single-frame regime under different multimodal fusion strategies. We analyze when RGB appearance is sufficient, when depth-derived geometric information provides consistent gains, and when semantic priors from action history dominate the prediction. Beyond the presence of each modality, we show that the fusion mechanism critically influences whether modalities reinforce or interfere with each other, and therefore we evaluate multiple fusion strategies.

We further consider two deployment-relevant factors. First, not all frames are equally informative: blur, occlusion, and viewpoint can severely affect performance, as observed in similar video understanding tasks [26], [27]. Accordingly, we study keyframe selection policies and their impact across different viewpoints. Second, action history priors are inherently noisy and imperfect, as they are derived from auxiliary predictive models. To address these limitations, we introduce a refinement mechanism that enhances robustness in practical settings through a stochastic corruption operator.

In this context, an additional question is how to obtain the semantic action history used as contextual prior. Recent progress in large language models (LLMs) and vision-language models (VLMs) suggests the possibility of inferring procedural structure or past actions directly from a single image [23], [28]. Motivated by the observation that humans can often infer plausible prior steps from a snapshot in structured environments, we compare histories inferred by modern VLMs [29], [30] with those produced by a single-frame action recognition model. Furthermore, we evaluate VLM-based histories under varying levels of prompt specificity and contextual information, in line with recent findings on the benefits of fine-grained prompting [31]–[33].

Based on these findings, we propose AAG+, an enhanced multimodal single-frame framework that consistently improves upon AAG through more robust modality selection and more effective fusion strategies, building on insights from multimodal transformer architectures [34], while preserving its efficiency advantages. Additionally, it achieves competitive performance with state-of-the-art video-based methods. Our contributions are summarized as follows:

- We conduct a systematic analysis of modality contributions in single-frame action anticipation, quantifying the impact of RGB appearance, depth-based geometric cues, and semantic past-action context.

- Building on these insights, we study multimodal fusion and frame-selection strategies and introduce AAG+, which combines the most effective modalities and design choices, yielding consistent improvements over AAG and competitive performance with state-of-the-art video-based methods.
- We further study the role of past action context in single-frame anticipation, comparing histories derived from an action recognition model with those inferred by VLMs under different prompts and levels of contextual information, analyzing their temporal consistency and reliability.

All findings are validated through extensive experiments on diverse procedural activity datasets (IKEA-ASM [5], Meccano [35], Assembly101 [4]), providing practical insights into when multimodal single-frame anticipation can serve as an effective alternative to dense video-based approaches. The implementation of AAG+ will be made publicly available¹.

The remainder of the paper is organized as follows. Section II reviews related work. Section III details the proposed framework design. Section IV describes the datasets and evaluation protocol. Section V reports the main results and ablations on modalities, fusion, keyframe selection, and robustness to imperfect histories. Section VI draws the main conclusions of this work.

II. RELATED WORK

We review existing approaches for multimodal video-based action anticipation, and subsequently concentrate on methods for single-frame action recognition and anticipation, due to the limited work in this area.

Video-based Human Action Anticipation has attracted significant attention in recent years [9]. Several approaches operate solely on RGB video inputs and achieve state-of-the-art results by leveraging effective temporal modeling strategies. Among them, TempAgg [11] proposes a versatile multi-scale temporal aggregation scheme aimed at tackling the complexities of long-range video understanding. Similarly, the Anticipative Video Transformer (AVT) [10] adopts an end-to-end attention-driven framework that simultaneously anticipates future actions and learns frame representations optimized for predicting forthcoming content. By explicitly maintaining the order of observed actions, AVT captures long-term temporal dependencies in a structured and principled way.

In contrast, multimodal methods leverage complementary information from multiple modalities to build more informative representations ahead of the classification stage. For example, in RULSTM [12], authors propose a Rolling-Unrolling LSTM for action anticipation. A Rolling LSTM encodes observed frames to capture temporal structure and an Unrolling LSTM forecasts future actions and object interactions. Textual cues, typically expressed as action descriptions, have also been shown to enhance anticipation. The Visual-Linguistic Modeling of Action History framework (VLMAH) [13] integrates immediate visual features with a lightweight linguistic representation of past actions, enabling the modeling of both short-term and long-term context.

¹<https://github.com/ManuBenavent/AAG-Plus>

The task of action anticipation has recently seen a paradigm shift with the integration of large language models and vision-language models to provide semantic priors and high-level reasoning. AntGPT [14] leverages the reasoning capabilities of large language models to extract goal-directed activities, often termed high-level actions, from video sequences. By treating these high-level goals as anchors, the model improves the prediction of upcoming fine-grained actions through a more structured understanding of intent. A similar strategy is employed in [15], where a joint loss function is introduced to enforce consistency between fine-grained future actions and coarse-grained goal predictions, ensuring that anticipated movements align with the overall objective of the actor. PlausiVL [16] extends the generative capabilities of video-language models by introducing a “plausibility” loss using counterfactual learning to distinguish between realistic and unrealistic action sequences, effectively acting as a semantic filter for future predictions. Moreover, the model proposed in [17] explicitly infers behavioral intentions as textual features before feeding them into an LLM for final sequence forecasting. On the other hand, BiAnt [36] introduces bidirectional action sequence learning by training the model to predict both forward (past to future) and backward (future to past), enforcing a stricter form of temporal continuity and goal-consistency. Finally, ActionLLM [37] further optimizes this paradigm by leveraging the role of VLMs as action anticipators. It treats video sequences as successive tokens, utilizing “action-tuning” to align the LLM’s internal knowledge with the specific constraints of the action anticipation domain.

Single-Frame Human Action Recognition remains a fundamentally difficult problem, primarily because the visual evidence is restricted to a single observation and thus lacks the temporal dynamics that typically disambiguate human activities. To compensate for this limitation, prior work has explored complementary strategies, including knowledge distillation, explicit contextual reasoning, and stronger feature learning mechanisms. Early efforts, such as [38], employ region-based CNN formulations that couple person-centric regions with informative environmental cues and highlight that accurate recognition often depends on jointly modeling the actor and the surrounding scene. More recent methods emphasize spatial reasoning and structured representation learning to better capture human-object interactions and scene semantics. Ashrafi et al. [39] explicitly model relationships between body joints and manipulated objects, aiming to represent interaction patterns that are indicative of the underlying action. Liang et al. [40] introduce a patch-based formulation that localizes actions in still images without requiring bounding-box supervision. In parallel, transformer-based architectures have been adopted to strengthen global reasoning over poses and contextual cues, leveraging vision transformers to extract spatial relations between human pose configurations and scene context [41]. Model efficiency and generalization have also been improved in [42], by proposing progressive knowledge distillation to transfer discriminative capacity into lighter models. Finally, other approaches, including [43], further enhance contextual reasoning in still images by combining pixel-level and region-

level attention mechanisms.

Single-Frame Human Action Anticipation has been relatively underexplored despite its computational advantages [44], including avoiding temporal aggregation and enabling stronger spatial feature learning when studied alongside video supervision [24]. Owing to the limited context available in a single image, existing solutions are largely multimodal. Lan et al. [45] introduce hierarchical “movemes”, a multi-level representation that captures human movement at different granularities to anticipate future actions from a single image or short clip. Vondrick et al. [46] propose a self-supervised model that predicts high-level future visual features from a single image and produces diverse outcomes to account for uncertainty. Recent vision-language approaches emphasize common-sense-driven contextualization rather than explicit action prediction. VisualCOMET [47] infers dynamic context by reasoning about prior events, intentions, and plausible future outcomes. Similarly, ActionCOMET [48] derives action-related common-sense knowledge (e.g., preconditions, outcomes, intentions, and sequences) using language models and annotated cooking videos. Although neither VisualCOMET nor ActionCOMET performs direct action anticipation, both provide semantic signals that can support downstream reasoning tasks. Finally, our previous work on action anticipation introducing AAG [25] explicitly addresses the challenge of predicting upcoming actions from a single moment. Unlike video-based models that require temporal aggregation, AAG leverages a single RGB frame enriched with depth cues and textual summaries to provide long-term context. Results demonstrate that semantic priors can compensate for the lack of temporal visual information.

III. MULTIMODAL REFINEMENT FOR ACTION ANTICIPATION AT A GLIMPSE

We revisit the core design of Action Anticipation at a Glimpse and present an enhanced version, AAG+, which addresses the limitations identified in the original framework. AAG+ refines modality processing through improved feature extractors, introduces a keyframe selection mechanism, and incorporates a stochastic corruption operator to handle imperfect action histories. We further provide a focused analysis of multimodality and fusion strategies, with all extensions guided by a systematic evaluation of individual component and modality contributions.

To structure the presentation, we organize it around the three main modules of AAG+: the visual encoder module, the action history retrieval module, and the multimodal fusion and classification module. In the following sections, we revisit each module, describe the original design, and highlight the specific refinements introduced in AAG+ to overcome the original limitations. An overview of the AAG+ framework is presented in Figure 2.

A. Visual Encoder

In the AAG framework, visual reasoning is constrained to a single observation, under the assumption that a single frame can encode sufficient information about the scene state when enriched with complementary modalities. Specifically,

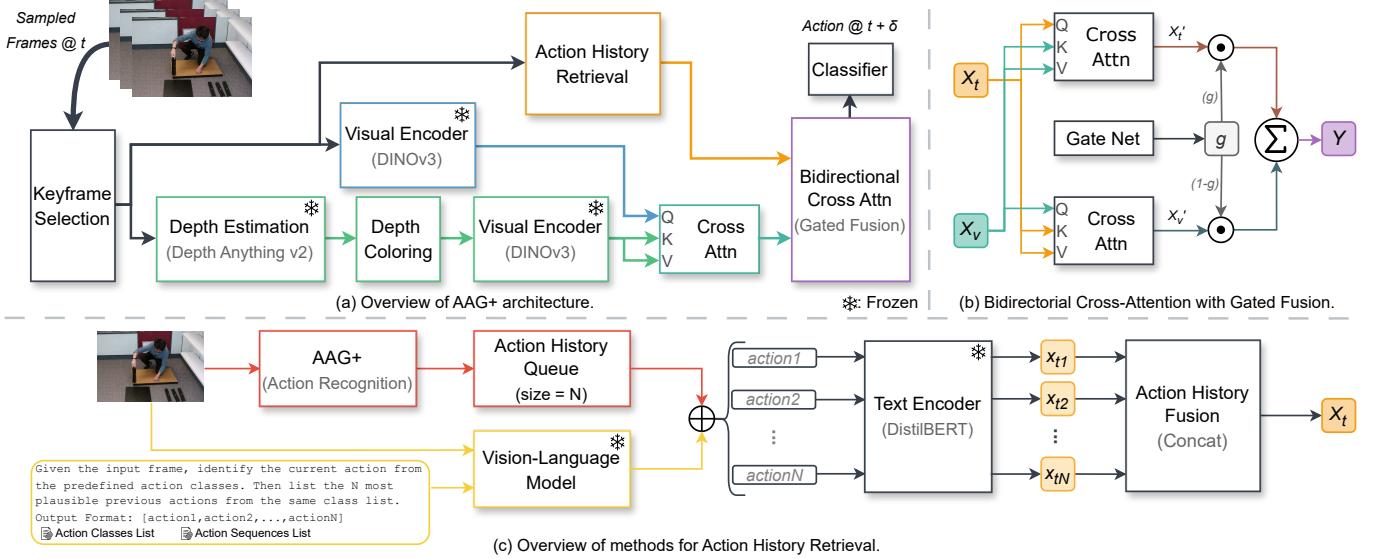


Fig. 2: **Illustration of AAG+.** (a) **Overview of AAG+ architecture.** Following keyframe selection, three modalities are processed. Depth (green) is estimated and colored prior to feature extraction and fusion with RGB features (blue). Visual fusion is performed via cross-attention, where RGB acts as the primary modality. Visual features are integrated with textual context (orange) extracted from the action history retrieval module through bidirectional cross-attention (purple). (b) **Bidirectional Cross-Attention with Gated Fusion.** Input features undergo independent cross-attention and are then combined through a gated fusion, where a learned gating vector g adaptively weights the contribution of each modality prior to summation. (c) **Overview of methods for Action History Retrieval.** We propose two methods for history retrieval: (yellow) prompting a VLM to predict the past actions sequence, or (red) repurposing the AAG+ architecture to perform action recognition on the current frame and storing the results in a queue of size N . In both cases, class names are mapped to a latent space via a text encoder to produce individual embeddings x_{tn} , which are subsequently fused into the joint representation X_t .

the encoder uses an RGB frame, f_t , and an aligned depth representation, d_t , from the last observed moment t to predict actions δ seconds into the future. RGB appearance features are extracted using a self-supervised vision transformer, originally DINOv2 [49], yielding $X_{\text{RGB}} \in \mathbb{R}^{D_{\text{vis}}}$, where D_{vis} denotes the feature dimensionality of the encoder. RGB features capture object appearance, layout, and actor-object interactions, but lack explicit geometric structure.

To complement appearance cues, AAG incorporates depth information, which provides explicit spatial relationships between scene elements. Since depth maps are single-channel and often noisy, depth is first estimated using a monocular depth model (Depth Anything v2 [50]) and converted into a pseudo-RGB representation via color mapping similar to [35]. This enables the use of the same feature extractor as for RGB, producing a depth embedding $X_{\text{D}} \in \mathbb{R}^{D_{\text{vis}}}$.

To integrate the two modalities, a cross-attention mechanism is employed in which RGB features act as queries and depth features as keys and values:

$$Q = W_Q X_{\text{RGB}}, \quad K = W_K X_{\text{D}}, \quad V = W_V X_{\text{D}}, \quad (1)$$

followed by the scaled dot-product attention operator:

$$X_V = \text{softmax} \left(\frac{QK^T}{\sqrt{D}} \right) V, \quad (2)$$

where $W_Q, W_K, W_V \in \mathbb{R}^{D \times D}$ are learnable projections and D denotes the shared embedding dimension. This formulation allows depth cues to selectively refine the RGB representation,

emphasizing spatially informative regions while preserving appearance-driven semantics.

In AAG+, we maintain this cross-attention strategy to fuse visual features. This decision is informed by previous results demonstrating that this approach outperforms alternatives such as self-attention. It is also supported by the multimodal analysis conducted in Section V, which reveals that limitations in visual reasoning reside in the input feature quality rather than in the fusion strategy itself.

Particularly, while the visual encoder proved effective in controlled exocentric settings (e.g. IKEA-ASM), we observe clear limitations in more challenging scenarios, where increased camera motion induces blur and frequent occlusions reduce object visibility, a common issue in egocentric or close-up view perspectives (e.g. Meccano, Assembly101). Under such conditions, the quality of the single observed frame becomes a dominant factor: noisy depth estimates and visually degraded RGB frames can overwhelm the cross-attention mechanism, limiting its ability to provide meaningful refinement.

Keyframe Selection. Motivated by these observations, we introduce refinements to the visual encoder that explicitly account for frame quality. Rather than strictly sampling the last frame, we adopt a keyframe selection strategy that prioritizes frames with low motion blur and high visual clarity. By ensuring that both RGB and depth features are extracted from visually informative frames, the cross-attention mechanism op-

erates on more reliable inputs, leading to improved robustness across datasets.

The keyframe selection module explicitly accounts for frame quality within a short temporal window into the past, set to five frames in our experiments. We evaluate three distinct keyframe selection strategies:

- **Blurriness-based Selection (Laplacian Variance):** We estimate the focus of each frame using the variance of the Laplacian. At each time step t , we examine the previous five frames, starting from the most recent frame f_t and moving backward. We select the first frame in this window whose Laplacian variance exceeds a predefined sharpness threshold. Should none of the frames meet the threshold, we default to f_t . Empirically, Laplacian variance over 300 indicates very sharp frames, 100–300 indicates sharp frames, 50–100 moderate blur, and under 50 pronounced motion blur. Thresholds are chosen per dataset based on viewpoint characteristics.
- **Distance-based Selection (L_2 and Cosine):** For each time step t , we extract RGB embeddings for all frames within the previous short-term window. We then compute the centroid of these embeddings and select the frame closest to this centroid as the most representative. This approach prioritizes frames that are semantically stable and representative of the recent temporal context.

AAG+ adopts blurriness-based keyframe selection as it outperforms distance-based strategies (see Section V) while significantly reducing computational overhead, as no feature extraction is required for the candidate frames.

Feature Extraction. In addition, we revisit the choice of visual backbone, which plays a critical role in the single-frame anticipation setting. When temporal redundancy is absent, the quality and robustness of the extracted visual representation directly constrain the model’s ability to reason about scene state and future actions. We therefore replace DINOv2 [49] with DINOv3 [51], which offers stronger representations and improved robustness to noise, motion blur, and appearance variation, which are factors that are particularly pronounced in unconstrained assembly scenarios.

We further explored more specialized depth-aware architectures, including Depth Anything 3 [52]. However, despite their suitability for dense geometric reasoning, these alternatives did not yield consistent improvements for single-frame anticipation compared to the one used in AAG, Depth Anything v2 [50]. As such, they are not adopted in the final model. Ablation results on the visual feature encoders are provided in Appendix A.

B. Action History Retrieval

Action anticipation is inherently ambiguous, particularly when relying on a single visual observation. In the absence of explicit temporal modeling, information about previously executed actions provides crucial context for disambiguating plausible futures. AAG addressed this challenge by representing past actions in textual form, motivated by prior work showing that long-term temporal dependencies can be effectively encoded using language-based representations [13], [53].

Building on this insight, within the AAG framework we explored using a single-frame action recognizer to obtain past actions, encoded either as free-form textual descriptions or as individual per-action embeddings. Experiments showed that representing each past action independently and aggregating the embeddings consistently outperformed encoding the entire history as a single summary. Motivated by these results and the ablations in AAG, we focus on independent action encodings aggregated via concatenation. This strategy is both more effective than alternative aggregation methods (e.g., self-attention), and computationally efficient: since action class names are known in advance, embeddings can be precomputed, avoiding the need to run a text encoder at inference time.

Formally, let $x_{tn} \in \mathbb{R}^{D_{\text{txt}}}$ denote the embedding of the n -th past action at time step t , obtained from the text encoder. The joint action history representation at time t is then computed as the concatenation of all N past action embeddings:

$$X_t = \text{Concat}(x_{t1}, x_{t2}, \dots, x_{tN}) \in \mathbb{R}^{N \cdot D_{\text{txt}}}. \quad (3)$$

The number of past actions N is determined empirically through ablation studies per dataset. The resulting representation X_t is subsequently projected into the joint embedding space, D , to be combined with visual features.

In AAG+, we retain this strategy and use DistilBERT [54] as the text encoder and explore two key extensions: (1) the source of action history and (2) robustness to imperfect histories. While AAG considered vision-language models producing textual descriptions, a direct comparison with independent action embeddings has not been studied. We evaluate recent VLMs [29], [30] and fine-grained prompting strategies [31]–[33] for this purpose. Additionally, since action histories are prone to noise due to reliance on auxiliary models (single-frame recognizers or VLMs), we introduce mechanisms to improve robustness under such conditions.

Action History Source. We evaluate two primary sources for constructing the action history:

- **VLM-based inference:** Inspired by the observation that humans can often infer prior steps from a single moment, particularly in structured environments, VLMs are used to reconstruct plausible past actions from a single frame. We evaluate state-of-the-art vision-language models (GPT 5.1 [30] and Gemini 3 [29]) under varying prompts, which differ in the level of detail in the instructions and the amount of contextual information provided, including class names, action sequences, and frequency of prior steps, among others. The number of past actions N is explicitly specified in the prompt, and model outputs are parsed into individual action class names. An example is shown in Figure 2.c, while full prompt specifications and qualitative results are provided in Appendix E.
- **Single-frame action recognizer:** Past actions are obtained from predictions of an action recognition model applied to the current frame, maintaining a queue of previously completed actions of size N under realistic inference conditions. This allows reuse of features already computed for action anticipation, providing an efficient, temporally grounded, and consistent action history representation.

Robustness to Imperfect Histories. No action history constructing method is immune to errors. To mitigate over-reliance on perfectly ordered ground-truth sequences observed during training, AGG+ introduces robustness mechanisms that encourage the model to handle imperfect histories. Specifically, we define a stochastic corruption operator $\mathcal{C}(\cdot)$ that transforms the joint history embedding X_T into a perturbed version \tilde{X}_T :

$$\tilde{X}_T = \mathcal{C}(X_T), \quad (4)$$

where \tilde{X}_T is used during training in place of X_T . Two instantiations of \mathcal{C} are considered:

- **Random embedding noise:** To increase robustness to small inaccuracies in the action history, the action history embedding, X_T , is stochastically perturbed during training using a combination of dropout and Gaussian noise. Each element of X_T is independently zeroed with probability p and rescaled by $1/(1-p)$:

$$\tilde{X}_T \leftarrow X_T \odot m/(1-p), \quad m_i \sim \text{Bernoulli}(1-p), \quad (5)$$

where \odot denotes element-wise multiplication.

Subsequently, Gaussian noise with standard deviation σ is added to the embeddings:

$$\tilde{X}_T \leftarrow \tilde{X}_T + \epsilon, \quad \epsilon \sim \mathcal{N}(0, \sigma^2 \mathbf{1}), \quad (6)$$

where $\mathbf{1}$ is a vector of ones matching the dimensionality of X_T . During the experiments, σ was set to 0.03.

- **Action swapping:** To simulate realistic errors in the action history rather than applying random noise to the whole embedding, each action in the sequence is independently replaced, with probability p , by a randomly selected alternative action from the dataset. Let x_{tn} denote the embedding of the n -th action, then, for each action:

$$x_{tn} \leftarrow \begin{cases} x'_{tn}, & \text{with probability } p, \\ x_{tn}, & \text{with probability } 1-p, \end{cases} \quad (7)$$

where x'_{tn} is the embedding of a randomly selected alternative action. This mechanism introduces both incorrect predictions and potential ordering inconsistencies while preserving the per-action embedding structure. Notably, the probability p is closely linked to the complexity of the dataset, the number of previous actions considered, N , and the accuracy of the action history retrieval method. Accordingly, we perform ablations on p for each dataset to identify the most effective settings.

C. Multimodal Fusion & Classification

Visual and textual cues are fused to form a global representation, Y , which is used for classification. In AAG, this fusion is performed using a self-attention mechanism, which was shown to outperform simpler strategies based on concatenation or element-wise arithmetic operations. However, the multimodal analysis presented in Section V reveals limitations in the ability of this mechanism to effectively integrate visual and textual embeddings.

For AAG+, we conducted an extensive study of attention-based fusion mechanisms to combine visual and textual feature spaces. Specifically, we evaluated cross-attention with residual and gated variants, bidirectional cross-attention with shared or independent weights, and alternative strategies for combining the resulting representations (e.g., concatenation, element-wise operations, self-attention, or gated fusion). Rather than listing all variants here, we focus on the top-performing configuration: bidirectional cross-attention with gated fusion, which integrates modality-specific representations through a learned gating mechanism (Fig. 2.b). Full descriptions and detailed comparisons of all variants are provided in Appendix A.

In this scheme, cross-modal interactions are extended beyond a single direction, allowing each modality to attend to the other. Formally, given visual and textual feature sequences X_v and X_t , we compute cross-attended representations in both directions by applying the cross-attention mechanism defined in Equations 1-2:

$$\begin{aligned} X'_v &= \text{CA}(Q = X_v, K = X_t, V = X_t), \\ X'_t &= \text{CA}(Q = X_t, K = X_v, V = X_v), \end{aligned} \quad (8)$$

where $\text{CA}(\cdot)$ denotes the cross-attention operation described previously. The resulting representations X'_v and X'_t are then combined via a gated fusion:

$$Y = g \odot X'_v + (1-g) \odot X'_t, \quad (9)$$

where $g \in [0, 1]$ is a learned gating vector that adaptively weights the contribution of each modality. This mechanism enables the model to integrate complementary information from both streams while modulating their influence according to reliability or relevance. The resulting representation $Y \in \mathbb{R}^D$ serves as the global feature for AAG+ and is fed to an MLP for classification using cross-entropy loss for supervision.

IV. EXPERIMENTAL SETUP

A. Datasets

We evaluate our approach on three publicly available datasets designed for action recognition and anticipation in industrial scenarios. They encompass diverse environments, action granularity levels, and procedural variability.

IKEA-ASM [5] contains third-person videos of furniture assembly featuring 33 atomic actions and 4 high-level activities. Following [25] we use the top RGB view and use the default environment-based train/test split.

Meccano [35] is an egocentric dataset comprising videos of participants assembling a toy motorbike, recorded with head-mounted sensors. It includes 61 action classes derived from 20 object and 12 verb categories. Following prior work [12], [13], [25], we use the standard 11/9 train/test split.

Assembly101 [4] contains videos of participants assembling and disassembling 101 toy vehicles without fixed instructions, resulting in diverse execution patterns. It includes over 1M action segments spanning 1380 fine-grained action classes, derived from 90 objects and 24 verbs, captured across 12 camera views. We use the exocentric (third-person) camera $v4$, which provides the best RGB performance [4], and follow

TABLE I: Comparison with state-of-the-art video-based action anticipation methods.

Action History (AH) is predicted by an action recognizer (single-frame for AAG & AAG+, video-based for VLMAH). Underline: best single-frame performance.

Method	Modalities	# Input Frames	IKEA-ASM		Meccano		Assembly101	
			Top-1/5 Acc	Recall@5	Top-1/5 Acc	Recall@5	Top-1/5 Acc	Recall@5
RULSTM [12]	RGB	14	26.37 / 70.05	16.00	24.08 / 58.23	22.38	5.95 / 21.28	1.00
TempAgg [11]	RGB	37	26.90 / 70.14	16.42	19.69 / 25.37	17.47	11.43 / 34.16	9.07
AVT [10]	RGB	10	27.10 / 69.70	45.78	27.43 / 53.38	32.05	7.25 / 23.80	17.03
VLMAH [13]	RGB, AH	8	52.31 / 85.44	47.45	29.11 / 57.05	57.05	9.17 / 27.63	25.13
AAG [25]	RGB-D, AH	1	44.66 / 82.87	46.59	26.43 / 54.95	12.27	13.46 / 32.87	9.80
AAG+	RGB-D, AH	1	<u>51.26 / 88.88</u>	54.78	<u>27.24 / 60.41</u>	16.12	13.14 / 32.28	<u>13.02</u>

the train/validation splits from [13], [25], as the official test set is not publicly available.

B. Methods & Implementation Details

Evaluation: We evaluate our method by predicting actions $\delta = 1s$ into the future and report performance using two standard metrics in action anticipation: top- k accuracy and class-mean Top-5 recall [4], [13], [35], [55]. Top- k accuracy captures uncertainty in future predictions, while class-mean Top-5 recall addresses long-tail class distributions. Following prior work, we adopt top- k accuracy as the primary metric for IKEA-ASM and Meccano [13], [35], and class-mean Top-5 recall for Assembly101 [4]. In the reported tables, bold font indicates the best performance for each dataset’s primary metric. To evaluate the role of action history, we report results using both ground-truth and predicted histories.

Experiments involving action recognition report top-1 accuracy following established benchmarks [4], [5], [35].

Implementation Details: We use DINOv3 [51] with ViT-7B/16 backbone pretrained on LVD-1689M and half-precision (FP16), and DistilBERT [54] as the visual and text encoders, respectively. Depth frames are estimated using Depth Anything v2 (Small) [50]. Transformer encoders consist of 2 layers, 4 attention heads per layer, and an embedding dimension $D = 768$. As described in Section III, AAG+ applies a cross-attention transformer for visual feature fusion, followed by a bidirectional cross-attention transformer with gated fusion for multimodal integration. Keyframe selection is based on Laplacian variance with a threshold of 100 on IKEA-ASM and Assembly101, and 50 for Meccano due to lower-quality frames (see Appendix A for quantitative and qualitative comparisons of frame blurriness per dataset). Action history is retrieved using a single-frame action recognizer, as determined by the ablation studies in the next section. Even though full results on the accuracy of the single-frame action recognizer are provided in Appendix B, we report key finding here. Using an RGB frame and action history, the model achieves 72.38% on IKEA-ASM, 33.19% on Meccano, and 30.74% on Assembly101. Adding depth yields: 72.95%, 33.79%, and 31.49%, respectively.

For experiments involving action history (AH), ground-truth sequences are used during training, while predicted sequences are used at inference. Following [25], the number of previous actions N is set to 7 for IKEA-ASM and 3 for Meccano and Assembly101. The action swapping strategy is employed to

simulate realistic errors, with swap probabilities p of 0.1 and 0.4 on IKEA-ASM and Meccano, respectively. Random noise is used on Assembly101 with $p = 0.1$ and noise distribution set to 0.03, as determined by the ablation study presented in the following section.

Training Details: AAG+ has been implemented using PyTorch, and experiments are conducted on Nvidia RTX 4090 GPUs. We employ AdamW optimizer with a weight decay of 0.01 and a base learning rate of 5×10^{-5} . Models are trained for 100 epochs, with an early stopping patience of 10 epochs, and an improvement threshold of 0.001. Batch size was set to 32.

SOTA Methods Details: We compare AAG+ with the original AAG framework, as well as four state-of-the-art video-based action anticipation methods, to assess the impact of single-frame versus video-based approaches. The methods include AVT [10], RULSTM [12], TempAgg [11], and VLMAH [13]. Missing baseline results reported in the original papers are taken from [25], which provides consistent train/test splits, camera views, and matched action history lengths.

V. EXPERIMENTAL RESULTS

A. Comparison to State-of-the-art Approaches

Table I compares the proposed multimodal single-frame model AAG+ with its predecessor, AAG, and with video-based (multi-frame) state-of-the-art action anticipation methods.

Despite using only a single frame, AAG+ outperforms several video-based methods and achieves competitive performance relative to approaches that rely on attention-based temporal modeling, such as AVT, and multimodal methods such as VLMAH. In particular, on IKEA-ASM, AAG+ performs comparably to the top-performing method VLMAH and outperforms RGB-only video-based approaches including TempAgg, AVT, and RULSTM, highlighting that strong spatial features and contextual priors can partially substitute for explicit temporal aggregation in structured tasks.

On more complex procedural datasets such as Meccano and Assembly101, where action sequences are longer, more variable, and less predictable, AAG+ remains competitive with video-based methods. These results indicate that even under higher temporal uncertainty, single-frame models can exploit strong spatial cues and local context to anticipate plausible next actions. At the same time, a performance gap remains relative to video-based approaches that explicitly model long-term dependencies through computationally heavier temporal

TABLE II: Effect of each modality on AAG+ across datasets and action history source (GT vs. Predictions). Underline: best per block. Bold: best under realistic settings. *: AH populated from AAG+’s action recognizer (RGB-D, AH).

AH Source	Modalities	IKEA-ASM		Meccano		Assembly101	
		Top-1/5 Acc	Recall@5	Top-1/5 Acc	Recall@5	Top-1/5 Acc	Recall@5
None	RGB	37.37 / 87.64	46.57	27.21 / 49.77	8.30	0.30 / 1.49	4.03
	RGB, Depth	<u>38.18 / 86.95</u>	48.75	<u>27.21 / 50.23</u>	8.33	0.32 / 1.65	3.85
GT	AH	63.55 / 94.52	65.09	31.75 / 73.57	37.33	31.19 / 59.70	<u>38.49</u>
	RGB, AH	62.38 / 94.04	65.73	31.00 / 71.83	32.68	28.74 / 56.19	33.80
	RGB, Depth, AH	<u>65.87 / 94.20</u>	64.05	<u>33.24 / 73.47</u>	35.17	30.34 / 57.81	36.66
Pred	AH*	48.02 / 87.56	53.58	26.43 / 59.81	17.32	13.14 / 32.28	13.02
	RGB, AH	48.90 / 89.32	56.34	26.85 / 58.11	14.39	12.57 / 30.20	10.97
	RGB, Depth, AH	51.26 / 88.88	54.78	27.24 / 60.41	16.12	12.49 / 30.81	12.89

mechanisms, such as AVT, or multimodal video-based methods such as VLMAH, although AAG+ consistently outperforms methods relying on dense frame aggregation alone, including RULSTM and TempAgg. Our results highlight the potential of single-frame reasoning in structured and predictable environments, while also revealing its limitations, as temporal modeling continues to provide an advantage in more flexible or ambiguous tasks. We further compare computational complexity in Appendix C to illustrate the efficiency advantages of single-frame anticipation over video-based approaches.

Compared to its predecessor, AAG+ consistently improves across all datasets. In addition to more robust visual features, refined keyframe selection mitigates AAG’s limitations with respect to viewpoint sensitivity. AAG+ also handles imperfect action histories more effectively through dedicated robustness mechanisms. Finally, AAG+ combines the available features more effectively, guided by the multimodal analysis presented in the next section.

B. Multimodal Complementarity Analysis

To examine how multimodal fusion and temporal context jointly influence anticipation performance under varying levels of dataset complexity and observation uncertainty, we analyze AAG+ from two complementary perspectives. First, we quantify the effect of different modality combinations under both idealized ground-truth and realistic predicted action-history settings. Second, we perform a per-sample analysis of visual and textual contributions to correct and incorrect predictions, revealing conditions under which the modalities act redundantly or complementarily.

1) *Effect of Modality Composition under Ground-Truth and Predicted Action Histories*: Table II analyzes the contribution of individual and combined modalities in AAG+ under two settings: ground-truth (GT) histories and realistic (Pred) histories populated by an equivalent single-frame action recognizer.

The analysis indicates that when no action history is available, RGB alone provides a reasonable baseline on IKEA-ASM and Meccano, while performing poorly on Assembly101, potentially attributed to the complexity and variability of the tasks in this dataset. Adding depth consistently improves or stabilizes performance across datasets, confirming that geometric cues complement RGB by providing spatial disambiguation, particularly in visually cluttered scenes.

Combining visual cues with action history further improves performance under both GT and predicted action history population settings. Using GT action history yields a substantial performance boost across all datasets, highlighting the importance of long-term procedural context. Under realistic settings, multimodality becomes even more critical. While predicted action history alone is noisy, fusing it with RGB stabilizes predictions, and incorporating depth further enhances robustness, leading to the best performance across all datasets according to their respective evaluation protocols.

From a dataset perspective, it is evident that the impact of multimodality is strongly modulated by dataset complexity. On IKEA-ASM, which features shorter procedural sequences and lower intra-activity variability, strong visual cues are often sufficient for action anticipation, and action history primarily acts as a performance booster. Consequently, gains from multimodal fusion are incremental. In contrast, for Meccano and especially Assembly101 which exhibit longer action sequences, a larger action vocabulary, and higher visual ambiguity at reliance on action history becomes increasingly critical. The textual action history encoder provides a strong procedural prior that helps disambiguate future actions when instantaneous visual evidence is insufficient. Under realistic conditions, multimodal fusion plays a compensatory role: while predicted action histories are imperfect, their integration with RGB and depth stabilizes anticipation by balancing short-term visual evidence with long-term task progression.

2) *Modality Contribution Analysis via Visual-Textual Agreement*: To better understand how different modalities contribute to anticipation performance on each dataset, following [56], we conduct a meta-analysis based on confusion matrix-style breakdowns that quantify, for each sample, whether the visual branch (RGB and depth), the textual action history branch, or both lead to a correct or incorrect prediction. This analysis goes beyond aggregate accuracy and reveals when modalities are complementary versus redundant.

Our analysis, shown in Figure 3, reveals that while the visual modality provides essential grounding in the physical scene, the text modality often stabilizes predictions, particularly under high visual occlusion or ambiguity, as in Meccano and Assembly101. For both the original AAG and the improved AAG+ models, the text modality contributes most strongly to overall performance, highlighting the importance of long-term procedural context, especially in datasets with many activities,

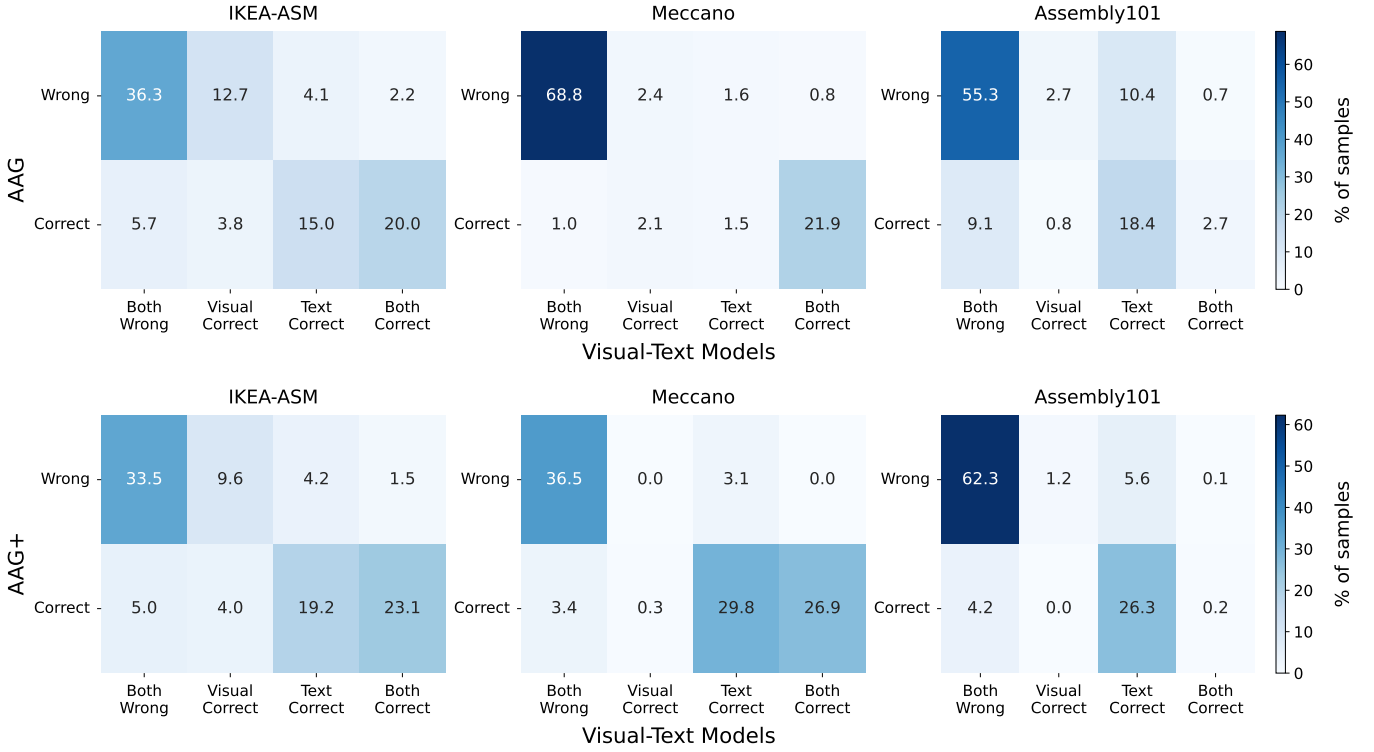


Fig. 3: **Confusion matrix-style modality breakdown for AAG and AAG+ across datasets.** Each sample is categorized by whether the visual branch (RGB-Depth), the text action-history branch, or both produce a correct prediction.

such as IKEA-ASM and Assembly101, and with high intra-activity variation, as in Assembly101.

Comparing AAG and AAG+, both models exhibit dataset-dependent modality preferences. Across all datasets, AAG+ consistently outperforms AAG by shifting probability mass from failure cases toward jointly correct multimodal predictions through its bidirectional cross-attention mechanism. On IKEA-ASM and Meccano, these gains are primarily driven by an increase in jointly correct predictions, indicating improved cross-modal agreement. On more complex datasets, especially Assembly101, AAG+ shows a higher proportion of *Text Correct* cases than AAG, reflecting the increased importance of robustness to imperfect action histories in settings with longer action sequences, higher intra-activity variation, and visually ambiguous intermediate states, where single-frame visual cues are often insufficient.

We further analyze the contributions of each modality and the effectiveness of the fusion mechanism in Appendix D under visual-only (RGB-Depth) and RGB-Text settings.

C. Impact of Keyframe Selection

Table III reports the impact of different keyframe selection strategies across IKEA-ASM, Meccano, and Assembly101 datasets. We compare uniform sampling of the most recent frame (*None*) against distance-based selection using cosine and L_2 similarity, as well as blurriness-based selection using the Laplacian variance.

Distance-based strategies are consistently outperformed by the blurriness-based strategy and, in most cases, by not apply-

ing any keyframe selection, likely due to noisy embeddings caused by motion blur. In contrast, blurriness-based selection consistently achieves the strongest or comparable performance across metrics. While absolute gains are modest, this approach improves robustness by avoiding visually degraded frames that can negatively affect both RGB and depth feature extraction.

As previously noted, IKEA-ASM and Assembly101 use a threshold of 100, considering frames with Laplacian variance above this value as sharp. As reported in Appendix A, the mean Laplacian on IKEA-ASM exceeds 300, indicating very sharp frames, so blurriness-based selection yields results comparable to no selection, as the third-person perspective already provides clear, informative frames. Assembly101, on the other hand, has a mean slightly above 100, and discarding frames below this threshold yields measurable improvement.

Finally, Meccano presents the greatest challenge for keyframe selection due to pronounced motion blur from a head-mounted egocentric camera, with a mean Laplacian below 50, indicating pronounced blur. After evaluating thresholds of 30, 50, and 100, we adopt 50, which balances the number of updates while preserving reasonably sharp frames.

Overall, results show that the benefit of keyframe selection depends on the dataset. When most frames are already clear, simply using the most recent frame works well. In settings with more motion blur, explicitly filtering out blurry frames helps improve single-frame anticipation performance.

TABLE III: Comparison of keyframe selection strategies.

Strategy	IKEA-ASM		Meccano		Assembly101	
	Acc@1/5	R@5	Acc@1/5	R@5	Acc@1/5	R@5
None	48.9/85.1	53.0	26.1/56.4	20.2	12.4/29.9	12.1
Cos	46.2/85.4	54.4	25.5/59.1	20.5	12.8/29.7	11.7
L2	46.4/84.6	54.6	25.1/57.2	18.9	12.4/30.7	12.4
Blur	48.9/85.1	53.0	26.4/56.8	19.3	12.2/30.0	12.6

D. Impact of Stochastic Action History Corruptions

Table IV summarizes the effect of different action history corruption strategies when action histories are populated using predicted actions from equivalent action recognizers, and frames selected using the blurriness-based strategy.

We observe that performance is strongly influenced by both dataset complexity and the size of the action space. On IKEA-ASM, action swapping with moderate corruption levels ($p = 0.1 - 0.2$) achieve the highest Top-1 accuracy, improving robustness while preserving informative temporal cues. In contrast, Meccano, which has an action space approximately twice as large as IKEA-ASM and relies on a less accurate single-frame action recognizer, benefits from increased variability. Accordingly, higher corruption levels for action swapping ($p = 0.3 - 0.5$) yield the best results.

Assembly101 exhibits a markedly different behavior. Due to its large number of activities (> 1000) and substantially higher intra- and inter-activity variability, action swapping tends to degrade performance. Instead, applying random embedding noise and dropout provides the strongest gains, suggesting that softer, continuous perturbations are better suited to handling the high ambiguity of this dataset.

E. Impact of Action History Source

Table V reports anticipation performance across various action history sources on the IKEA-ASM dataset. This ablation is conducted without action history corruption strategies to isolate the impact of the source itself. We compare histories constructed by a single-frame action recognizer against those generated by GPT-5.1 and Gemini 3 Flash, utilizing varying degrees of contextual information (i.e., short vs. long prompts and sequences, as detailed in Section III). IKEA-ASM was selected for this analysis as its relatively lower task complexity provides a clear baseline for evaluating VLM-based history construction.

Results demonstrate that Gemini 3 Flash outperforms GPT 5.1, while also confirming that accuracy scales with context, a finding consistent with prior literature [31]–[33]. Despite this improvement, both VLM-based histories remain significantly inferior to the single-frame action recognizer.

Qualitative analyses in Appendix E reveal that, while VLMs provide plausible rationales for their predictions, they rely heavily on heuristic priors of common scenarios rather than on precise visual perception. This behavior is consistent with observations in [28] for video question-answering tasks. As

TABLE IV: Comparison of stochastic action history corruption strategies.

Strategy	IKEA-ASM		Meccano		Assembly101	
	Acc@1/5	R@5	Acc@1/5	R@5	Acc@1/5	R@5
None	48.9/85.1	53.0	26.4/56.8	19.3	12.2/30.0	12.6
Noise	49.8/88.4	56.4	26.2/58.0	16.9	12.5/30.8	12.9
Swap $p = 0.1$	51.3/88.9	54.8	24.8/59.1	17.0	12.2/30.9	12.0
Swap $p = 0.2$	51.2/89.7	54.2	26.1/57.9	17.5	12.2/32.0	12.5
Swap $p = 0.3$	50.1/89.9	59.1	27.2/60.4	16.1	12.8/32.4	12.1
Swap $p = 0.4$	48.0/89.2	56.9	26.9/61.3	15.9	12.5/33.0	12.3
Swap $p = 0.5$	47.0/87.6	53.3	26.8/60.7	15.9	12.9/34.2	11.6

TABLE V: Comparison of action history sources.

Source	Top1/5	Acc	Rec@5
Single-Frame Action Recognizer	48.90	94.20	64.05
GPT 5.1 (Short Prompt)	14.37	54.14	28.18
GPT 5.1 (Long Prompt)	17.45	55.66	27.83
GPT 5.1 (Long + Action Seq)	15.45	53.34	26.57
Gemini 3 Flash (Short Prompt)	19.05	68.27	36.62
Gemini 3 Flash (Long Prompt)	20.45	67.47	35.54
Gemini 3 Flash (Long + Action Seq)	22.89	71.67	42.16

a result, action history retrieval is biased toward typical behaviors rather than the specific assembly instructions, which in turn negatively affects anticipation performance, strongly dependent on the accuracy of the action history.

VI. CONCLUSIONS

In this work, we investigated action anticipation under the extreme constraint of single-frame observation, aiming to understand how far performance can be pushed when instantaneous visual cues are combined with structured temporal priors. Building on our previous AAG framework, we introduce AAG+, which incorporates improved keyframe selection, more reliable action-history modeling, robustness to imperfect histories, and more effective multimodal fusion. Our experiments across datasets of increasing complexity show that AAG+ consistently outperforms AAG by shifting predictions away from failure cases toward joint visual-textual correctness.

A central finding is that, when equipped with state-of-the-art single-frame foundation models for appearance and geometry, single-frame anticipation can approach, and in some cases surpass, the performance of methods that explicitly process full video clips. This indicates that much of the information exploited by video-based models is implicitly captured by strong per-frame representations, provided that long-term procedural context is explicitly encoded and leveraged. The relative contribution of modalities is strongly dataset-dependent: visual cues dominate in short, visually unambiguous procedures, while textual action-history representations gain importance in long-horizon, high-variability settings. Crucially, AAG+ learns to adapt its reliance on visual versus textual cues rather than enforcing a fixed modality hierarchy.

Beyond performance gains, this work offers empirical insight into the limits and capabilities of single-frame anticipation. It demonstrates that, with modern foundation models

and principled multimodal fusion, single-frame approaches provide a competitive and computationally efficient alternative to video-based methods, particularly in low-latency settings where multi-frame processing is impractical. These findings offer a foundation for future research on anticipation, procedural reasoning, and decision-making under partial observability.

ACKNOWLEDGMENTS

This work has been funded by the Spanish State Research Agency (AEI) and ERDF/EU under grant: GEMELIA PID2024-161711OB-I00. This work has also been supported by a Spanish national fund for PhD studies, (FPU21/00414) as well as by the European Union (EU - HE Magician – Grant Agreement 101120731).

REFERENCES

- [1] A. Rasouli, I. Kotseruba, and J. K. Tsotsos, “Pedestrian action anticipation using contextual feature fusion in stacked rnns,” *BMVC*, 2020.
- [2] B. Liu, E. Adeli, Z. Cao, K.-H. Lee, A. Shenoi, A. Gaidon, and J. C. Nibbles, “Spatiotemporal relationship reasoning for pedestrian intent prediction,” *IEEE Robotics and Automation Letters*, vol. 5, no. 2, pp. 3485–3492, 2020.
- [3] H. Girase, H. Gang, S. Malla, J. Li, A. Kanehara, K. Mangalam, and C. Choi, “Loki: Long term and key intentions for trajectory prediction,” in *Proceedings of the IEEE/CVF International Conference on Computer Vision*, 2021, pp. 9803–9812.
- [4] F. Sener, D. Chatterjee, D. Shelepov, K. He, D. Singhania, R. Wang, and A. Yao, “Assembly101: A large-scale multi-view video dataset for understanding procedural activities,” in *Proceedings of the IEEE/CVF Conference on Computer Vision and Pattern Recognition (CVPR)*, June 2022, pp. 21 096–21 106.
- [5] Y. Ben-Shabat, X. Yu, F. Saleh, D. Campbell, C. Rodriguez-Opazo, H. Li, and S. Gould, “The ikea asm dataset: Understanding people assembling furniture through actions, objects and pose,” in *Proceedings of the IEEE/CVF Winter Conference on Applications of Computer Vision (WACV)*, January 2021, pp. 847–859.
- [6] J. Jang, D. Kim, C. Park, M. Jang, J. Lee, and J. Kim, “Etri-activity3d: A large-scale rgb-d dataset for robots to recognize daily activities of the elderly,” in *2020 IEEE/RSJ International Conference on Intelligent Robots and Systems (IROS)*. IEEE, 2020, pp. 10990–10997.
- [7] H. Hwang, C. Jang, G. Park, J. Cho, and I.-J. Kim, “Eldersim: A synthetic data generation platform for human action recognition in eldercare applications,” *IEEE Access*, vol. 11, pp. 9279–9294, 2021.
- [8] R. Dai, S. Das, S. Sharma, L. Minciullo, L. Garattoni, F. Bremond, and G. Francesca, “Toyota smarthome untrimmed: Real-world untrimmed videos for activity detection,” *IEEE Transactions on Pattern Analysis and Machine Intelligence*, vol. 45, no. 2, pp. 2533–2550, 2022.
- [9] B. Lai, S. Toyer, T. Nagarajan, R. Girdhar, S. Zha, J. M. Rehg, K. Kitani, K. Grauman, R. Desai, and M. Liu, “Human action anticipation: A survey,” *arXiv preprint arXiv:2410.14045*, 2024.
- [10] R. Girdhar and K. Grauman, “Anticipative video transformer,” in *Proceedings of the IEEE/CVF international conference on computer vision*, 2021, pp. 13 505–13 515.
- [11] F. Sener, D. Singhania, and A. Yao, “Temporal aggregate representations for long-range video understanding,” in *Computer Vision—ECCV 2020: 16th European Conference, Glasgow, UK, August 23–28, 2020, Proceedings, Part XVI 16*. Springer, 2020, pp. 154–171.
- [12] A. Furnari and G. M. Farinella, “Rolling-unrolling lstms for action anticipation from first-person video,” *IEEE transactions on pattern analysis and machine intelligence*, vol. 43, no. 11, pp. 4021–4036, 2020.
- [13] V. Manousaki, K. Bacharidis, K. Papoutsakis, and A. Argyros, “Vlmah: Visual-linguistic modeling of action history for effective action anticipation,” in *Proceedings of the IEEE/CVF International Conference on Computer Vision (ICCV) Workshops*, October 2023, pp. 1917–1927.
- [14] Q. Zhao, S. Wang, C. Zhang, C. Fu, M. Q. Do, N. Agarwal, K. Lee, and C. Sun, “Antgpt: Can large language models help long-term action anticipation from videos?” *ICLR*, 2024.
- [15] O. Zatsarynna and J. Gall, “Action anticipation with goal consistency,” in *2023 IEEE International Conference on Image Processing (ICIP)*. IEEE, 2023, pp. 1630–1634.
- [16] H. Mittal, N. Agarwal, S.-Y. Lo, and K. Lee, “Can’t make an omelette without breaking some eggs: Plausible action anticipation using large video-language models,” in *2024 IEEE/CVF Conference on Computer Vision and Pattern Recognition (CVPR)*, 2024, pp. 18 580–18 590.
- [17] C. Cao, L. Hu, Y. Yu, and Y. Zhang, “Vision and intention boost large language model in long-term action anticipation,” *arXiv preprint arXiv:2505.01713*, 2025.
- [18] W. Guo and Y. Kong, “Towards object-centric understanding for instructional videos,” *arXiv preprint arXiv:2512.03479*, 2025.
- [19] C. Zhang, C. Fu, S. Wang, N. Agarwal, K. Lee, C. Choi, and C. Sun, “Object-centric video representation for long-term action anticipation,” in *Proceedings of the IEEE/CVF Winter Conference on Applications of Computer Vision*, 2024, pp. 6751–6761.
- [20] S. V. Kodathala and R. Vunnam, “Temporal vs. spatial: Comparing dinov3 and v-jepa2 feature representations for video action analysis,” *arXiv preprint arXiv:2509.21595*, 2025.
- [21] L. Doorenbos, F. Spurio, and J. Gall, “Video panels for long video understanding,” *arXiv preprint arXiv:2509.23724*, 2025.
- [22] R. Yang, T. Yun, Z. Wang, and E. Pavlick, “Video finetuning improves reasoning between frames,” *arXiv preprint arXiv:2511.12868*, 2025.
- [23] Y. Zhou, L. Li, S. Qiu, Z. Yang, Y. Zhao, S. Han, Y. He, K. Li, H. Ji, Z. Zhao *et al.*, “Glimpse: Do large vision-language models truly think with videos or just glimpse at them?” in *Proceedings of the 2025 Conference on Empirical Methods in Natural Language Processing*, 2025, pp. 27 830–27 844.
- [24] J. Lei, T. L. Berg, and M. Bansal, “Revealing single frame bias for video-and-language learning,” *arXiv preprint arXiv:2206.03428*, 2022.
- [25] M. Benavent-Lledo, K. Bacharidis, V. Manousaki, K. Papoutsakis, A. Argyros, and J. Garcia-Rodriguez, “Action anticipation at a glimpse: To what extent can multimodal cues replace video?” in *Proceedings of the IEEE/CVF Winter Conference on Applications of Computer Vision (WACV) 2026*, 2026.
- [26] G. Sun, A. Singhal, B. Uz Kent, M. Shah, C. Chen, and G. Kessler, “From frames to clips: Training-free adaptive key clip selection for long-form video understanding,” *arXiv preprint arXiv:2510.02262*, 2025.
- [27] H. Liang, J. Li, T. Bai, X. Huang, L. Sun, Z. Wang, C. He, B. Cui, C. Chen, and W. Zhang, “Keyvideollm: Towards large-scale video keyframe selection,” *arXiv preprint arXiv:2407.03104*, 2024.
- [28] D. Ahn, Y. Choi, H. Choi, S. Cho, S. Kim, and J. Choi, “What happens when: Learning temporal orders of events in videos,” *arXiv preprint arXiv:2512.08979*, 2025.
- [29] G. Team *et al.*, “Gemini: a family of highly capable multimodal models,” *arXiv preprint arXiv:2312.11805*, 2023.
- [30] A. Singh *et al.*, “Openai gpt-5 system card,” *arXiv preprint arXiv:2601.03267*, 2025.
- [31] M. Wang, Z. Huang, X. Kong, G. Shen, G. Dai, J. Wang, and Y. Liu, “Action detail matters: Refining video recognition with local action queries,” in *Proceedings of the Computer Vision and Pattern Recognition Conference*, 2025, pp. 19 132–19 142.
- [32] Z. Yuan, X. Qu, C. Qian, R. Chen, J. Tang, L. Sun, X. Chu, D. Zhang, Y. Wang, Y. Cai *et al.*, “Video-star: Reinforcing open-vocabulary action recognition with tools,” *arXiv preprint arXiv:2510.08480*, 2025.
- [33] S. Zou, X. Tian, L. Wesemann, F. Waschowski, Z. Yang, and J. Zhang, “Unlocking vision-language models for video anomaly detection via fine-grained prompting,” *arXiv preprint arXiv:2510.02155*, 2025.
- [34] P. Xu, X. Zhu, and D. A. Clifton, “Multimodal learning with transformers: A survey,” *IEEE Transactions on Pattern Analysis and Machine Intelligence*, vol. 45, no. 10, pp. 12 113–12 132, 2023.
- [35] F. Ragusa, A. Furnari, and G. M. Farinella, “Meccano: A multimodal egocentric dataset for humans behavior understanding in the industrial-like domain,” *Computer Vision and Image Understanding*, vol. 235, p. 103764, 2023.
- [36] Y. Sato, Y. Ishii, and T. Yamashita, “Bidirectional action sequence learning for long-term action anticipation with large language models,” in *2025 19th International Conference on Machine Vision and Applications (MVA)*. IEEE, 2025, pp. 1–6.
- [37] B. Wang, Y. Tian, S. Wang, and L. Yang, “Multimodal large models are effective action anticipators,” *IEEE Transactions on Multimedia*, 2025.
- [38] G. Gkioxari, R. Girshick, and J. Malik, “Contextual action recognition with r* cnn,” in *Proceedings of the IEEE international conference on computer vision*, 2015, pp. 1080–1088.
- [39] S. S. Ashrafi, S. B. Shokouhi, and A. Ayatollahi, “Still image action recognition based on interactions between joints and objects,” *Multimedia Tools and Applications*, vol. 82, no. 17, pp. 25 945–25 971, 2023.
- [40] S. Liang, J. Wang, and Z. Zhuang, “Patch excitation network for boxless action recognition in still images,” *The Visual Computer*, vol. 40, no. 6, pp. 4099–4113, 2024.

- [41] S. R. Hosseini, S. Seyedin, and H. Taheri, "Human action recognition in still images using convit," in *2024 32nd International Conference on Electrical Engineering (ICEE)*. IEEE, 2024, pp. 1–7.
- [42] A. H. Saleknia and A. Ayatollahi, "Multi step knowledge distillation framework for action recognition in still images," in *2024 20th CSI International Symposium on Artificial Intelligence and Signal Processing (AISP)*. IEEE, 2024, pp. 1–7.
- [43] J. He, W. Wu, and Y. Li, "Context enhancement methodology for action recognition in still images," in *International Conference on Artificial Neural Networks*. Springer, 2023, pp. 112–122.
- [44] T.-H. Vu, C. Olsson, I. Laptev, A. Oliva, and J. Sivic, "Predicting actions from static scenes," in *Computer Vision – ECCV 2014*, D. Fleet, T. Pajdla, B. Schiele, and T. Tuytelaars, Eds. Cham: Springer International Publishing, 2014, pp. 421–436.
- [45] T. Lan, T.-C. Chen, and S. Savarese, "A hierarchical representation for future action prediction," in *Computer Vision–ECCV 2014: 13th European Conference, Zurich, Switzerland, September 6–12, 2014, Proceedings, Part III 13*. Springer, 2014, pp. 689–704.
- [46] C. Vondrick, H. Pirsiavash, and A. Torralba, "Anticipating visual representations from unlabeled video," in *Proceedings of the IEEE conference on computer vision and pattern recognition*, 2016, pp. 98–106.
- [47] J. S. Park, C. Bhagavatula, R. Mottaghi, A. Farhadi, and Y. Choi, "Visualcomet: Reasoning about the dynamic context of a still image," in *Computer Vision–ECCV 2020: 16th European Conference, Glasgow, UK, August 23–28, 2020, Proceedings, Part V 16*. Springer, 2020, pp. 508–524.
- [48] S. K. Sampat, Y. Yang, and C. Baral, "Actioncomet: A zero-shot approach to learn image-specific commonsense concepts about actions," *arXiv preprint arXiv:2410.13662*, 2024.
- [49] M. Oquab, T. Darcet, T. Moutakanni, H. Vo, M. Szafraniec, V. Khalidov, P. Fernandez, D. Haziza, F. Massa, A. El-Nouby *et al.*, "Dinov2: Learning robust visual features without supervision," *arXiv preprint arXiv:2304.07193*, 2023.
- [50] L. Yang, B. Kang, Z. Huang, Z. Zhao, X. Xu, J. Feng, and H. Zhao, "Depth anything v2," in *Advances in Neural Information Processing Systems*, A. Globerson, L. Mackey, D. Belgrave, A. Fan, U. Paquet, J. Tomczak, and C. Zhang, Eds., vol. 37. Curran Associates, Inc., 2024, pp. 21 875–21 911.
- [51] O. Siméoni, H. V. Vo, M. Seitzer, F. Baldassarre, M. Oquab, C. Jose, V. Khalidov, M. Szafraniec, S. Yi, M. Ramamonjisoa *et al.*, "Dinov3," *arXiv preprint arXiv:2508.10104*, 2025.
- [52] H. Lin, S. Chen, J. Liew, D. Y. Chen, Z. Li, G. Shi, J. Feng, and B. Kang, "Depth anything 3: Recovering the visual space from any views," *arXiv preprint arXiv:2511.10647*, 2025.
- [53] M. Benavent-Lledo, D. Mulero-Pérez, D. Ortiz-Perez, J. Garcia-Rodríguez, and A. Argyros, "Enhancing action recognition by leveraging the hierarchical structure of actions and textual context," *Computer Vision and Image Understanding*, vol. 262, p. 104560, 2025.
- [54] V. Sanh, L. Debut, J. Chaumond, and T. Wolf, "Distilbert, a distilled version of bert: smaller, faster, cheaper and lighter," *arXiv preprint arXiv:1910.01108*, 2019.
- [55] D. Damen, H. Doughty, G. M. Farinella, A. Furnari, E. Kazakos, J. Ma, D. Moltisanti, J. Munro, T. Perrett, W. Price *et al.*, "Rescaling egocentric vision: Collection, pipeline and challenges for epic-kitchens-100," *International Journal of Computer Vision*, pp. 1–23, 2022.
- [56] K. Kontras, T. Strypsteen, C. Chatzichristos, P. P. Liang, M. B. Blaschko, and M. De Vos, "Balancing multimodal training through game-theoretic regularization," in *The Thirty-ninth Annual Conference on Neural Information Processing Systems*, 2025.
- [57] J. Carreira and A. Zisserman, "Quo vadis, action recognition? a new model and the kinetics dataset," in *proceedings of the IEEE Conference on Computer Vision and Pattern Recognition*, 2017, pp. 6299–6308.
- [58] C. Feichtenhofer, H. Fan, J. Malik, and K. He, "Slowfast networks for video recognition," in *Proceedings of the IEEE/CVF International Conference on Computer Vision (ICCV)*, October 2019.
- [59] J. Lin, C. Gan, and S. Han, "Tsm: Temporal shift module for efficient video understanding," in *Proceedings of the IEEE/CVF International Conference on Computer Vision*, 2019, pp. 7083–7093.



Manuel Benavent-Lledo received his B.Sc. in Computer Science and M.Sc. in Automation and Robotics from the University of Alicante, Spain (2021, 2022), and his PhD in deep learning and computer vision from the University of Alicante in 2025. He is currently a postdoctoral researcher at the Department of Computer Technology, University of Alicante. His research interests include computer vision and deep learning for human action understanding and multimodal fusion.



Konstantinos Bacharidis received his B.Sc. and M.Sc. from the School of Electrical and Computer Engineering, Technical University of Crete (2014, 2016), and his Ph.D. in Computer Science from the University of Crete (2024), where he is a postdoctoral researcher. He is affiliated with the Human-Centered Computer Vision group at the Computational Vision and Robotics Laboratory, FORTH. His research focuses on human action recognition, anticipation, and error detection.

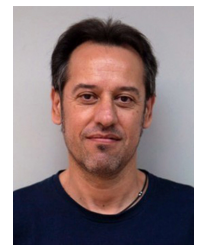


Konstantinos Papoutsakis is a postdoctoral researcher at the Institute of Computer Science, FORTH, in Heraklion, Crete, Greece. He earned his diploma in Computer Engineering and Informatics from the University of Patras in Greece in 2007, his M.Sc. and PhD degrees in Computer Science from the University of Crete in 2010 and 2019, respectively. His main research interests fall in the areas of computer vision, machine learning and visual perception for robotics with emphasis on human motion analysis, video segmentation, action segmentation,

and recognition, and human-computer and human-robot interaction. He has also been actively involved in several EU-funded projects as a computer vision engineer during his postgraduate studies. He has served as PI for a two-year research project (InterLink) funded by the Hellenic Foundation for Research and Innovation (HFRI).



Antonis Argyros is a professor of computer science at the Computer Science Department, University of Crete and a researcher at the Institute of Computer Science, FORTH, in Heraklion, Crete, Greece. His current research interests fall in the areas of computer vision and pattern recognition, with emphasis on human body pose and shape analysis and on the recognition of human gestures, actions, activities and intentions. He is also interested in applications of computer vision in the fields of robotics and smart environments.



Jose Garcia-Rodríguez received his Ph.D. degree, with specialization in Computer Vision and Neural Networks, from the University of Alicante (Spain). He is currently Full Professor at the Department of Computer Technology of the University of Alicante. His research areas of interest include: computer vision, computational intelligence, machine learning, pattern recognition, robotics, man-machine interfaces, ambient intelligence, computational chemistry, and parallel and multicore architectures.

Understanding Multimodal Complementarity for Single-Frame Action Anticipation

Supplementary Material

The supplementary material is organized as follows. Appendix A presents a comprehensive ablation study on the impact of different fusion strategies and feature extractors, as well as an analysis of blurriness per dataset. Appendix B reports action recognition results for each dataset under different input features and compares them with existing baselines. Appendix C provides a comparison of AAG+ with state-of-the-art methods in terms of computational efficiency. Finally, Appendix E presents qualitative results for prompting strategies on vision-language models under the different strategies described in the main paper.

APPENDIX A ABLATION EXPERIMENTS

As discussed in the main paper, our goal is to enhance the method proposed in [25] by improving both the unimodal representations (RGB, Depth, Text) and their multimodal integration. To this end, we perform ablation studies on the IKEA-ASM dataset, analyzing different multimodal fusion strategies and evaluating the effectiveness of various feature extractors.

A. Multimodal Fusion

The original analysis in [25] showed that fusing RGB and depth through a cross-attention mechanism, where RGB queries attend to depth, is an effective way to inject geometric cues into the visual representation. This geometry-enhanced RGB embedding outperformed simpler fusion strategies such as concatenation, summation, mean fusion, or self-attention. The same paper also explored visual-textual fusion strategies based on simple operators, including concatenation, summation, mean fusion, and self-attention over visual and textual tokens. Among these, self-attention was the most effective. However, the multimodal analysis shows that it still fails in several multimodal cases: the model produces correct predictions when using visual or textual features independently, yet degrades when both modalities are combined. This inconsistency motivates our exploration of more expressive, modality-aware fusion mechanisms. Results are presented in Table S.I. Note that we evaluate under predicted action histories only those variants that showed the most promising performance under the perfect (GT) setting and that the visual feature is DINOv2 [49], as in the original AAG framework.

Self-Attention Baseline. We begin by revisiting the self-attention fusion module used in AAG, which serves as the baseline for our analysis. Let X_v and X_t denote the visual and textual feature sequences, respectively. The concatenated feature sequence is then

$$X = [X_v; X_t]. \quad (10)$$

The module computes queries, keys, and values via learned projections:

$$Q = W_Q X, \quad K = W_K X, \quad V = W_V X. \quad (11)$$

The fused representation is then obtained through the standard attention operator:

$$X' = \text{softmax}\left(\frac{QK^\top}{\sqrt{D}}\right)V, \quad (12)$$

where D denotes the feature dimensionality. Although effective in most cases, this mechanism does not adequately control all interactions across modalities and therefore exhibits limited fusion behavior in the visual-textual setting.

Cross-Attention. To introduce directional, modality-aware interactions, we compute the queries, keys, and values for cross-modal fusion as:

$$Q = W_Q X_{\text{src}}, \quad K = W_K X_{\text{tgt}}, \quad V = W_V X_{\text{tgt}}, \quad (13)$$

where X_{src} and X_{tgt} denote the source and target modalities (visual or textual). This asymmetric formulation allows one modality to attend to the other. Throughout this section, we refer to each configuration by the source of the queries, e.g., $\text{CA}(Q = X_t)$ or $\text{CA}(Q = X_v)$.

Results in the second block of Table S.I show that using the visual modality as source is significantly less effective under ground-truth action histories. In contrast, the configuration $\text{CA}(Q = X_t)$ yields much stronger performance, confirming that complementing textual representations with visual cues is the more informative direction of fusion. However, this advantage diminishes under predicted action histories, where errors from the single-frame action recognizer propagate into the textual embeddings, causing a noticeable drop in accuracy.

To mitigate this sensitivity, we further refine the cross-attention module by introducing *residual cross-attention*, which integrates the source modality with the attended representation. Formally, given the attended output X' (as defined in Equation 12) and the source modality X_{src} , we evaluate several fusion operators of the form:

$$Y = f(X_{\text{src}}, X'), \quad (14)$$

including additive residuals, mean fusion, element-wise products, and gated combinations. Among these, the gated variant introduces a learnable interpolation between the original and the attended representation:

$$Y = g \odot X_{\text{src}} + (1 - g) \odot X', \quad (15)$$

where $g \in [0, 1]$ is a learned scalar or vector gate.

These mechanisms aim to stabilize the fusion process by preserving modality-specific information while still benefiting

TABLE S.I: Comparison of multimodal fusion strategies on IKEA-ASM.

SA = Self-Attention; CA = Cross-Attention; Bi-CA = Bidirectional Cross-Attention.

Fusion Strategy	GT Action History		Preds Action History	
	Top-1/5 Acc	Recall@5	Top-1/5 Acc	Recall@5
SA (Baseline)	61.83 / 89.64	51.37	44.66 / 82.87	46.59
CA (Q = Visual)	37.94 / 81.79	40.00	-	-
CA (Q = Text)	64.03 / 94.24	64.70	40.42 / 78.71	49.48
Residual CA (Sum)	64.83 / 94.64	64.28	40.74 / 79.03	50.54
Residual CA (Mean)	64.39 / 94.44	63.81	-	-
Residual CA (Product)	<u>64.95 / 94.28</u>	64.53	40.10 / 79.47	49.79
Residual CA (Gated)	63.55 / 94.20	63.50	-	-
Cross-Residual	57.90 / 89.80	58.94	-	-
Gated Cross-Residual	<u>61.14 / 92.40</u>	56.02	-	-
Bi-CA Concat (Independent)	62.83 / 93.16	62.67	-	-
Bi-CA Concat (Shared Weights)	57.78 / 89.20	53.70	-	-
Bi-CA (Sum)	59.34 / 90.56	53.11	-	-
Bi-CA (Mean)	60.02 / 91.04	59.49	-	-
Bi-CA (Product)	62.18 / 91.28	55.50	-	-
Bi-CA (Gated)	<u>64.51 / 94.28</u>	62.30	45.82 / 83.27	52.64
Bi-CA (SA)	61.14 / 90.36	56.53	-	-

from cross-modal interaction. Nonetheless, the lack of information independent of the action recognizer accuracy hinders the performance of the model under a realistic setting, with the self-attention baseline providing stronger results than the evaluated approaches.

Cross-Residual Attention. To further explore lightweight cross-modal interactions, we consider *cross-residual attention* modules, which replace the attention operator with simple feature mixing between modalities. Given the attended output X' obtained from a directional cross-attention step, cross-residual fusion is defined as:

$$Y = X_{\text{tgt}} + X'. \quad (16)$$

This additive shortcut enables a direct injection of complementary cues without requiring a full attention layer.

In practice, we evaluate only the most informative configuration from the previous analysis, namely $CA(Q = X_t)$. In this case, the textual queries attend to the visual features, producing an attended representation, X'_t , that is then injected into the visual stream via

$$Y = X_v + X'_t. \quad (17)$$

This applies the residual fusion in the direction that gave the strongest cross-modal signal under ground-truth action histories.

Although the gated variant yields a modest improvement over the standard cross-residual fusion, both approaches perform worse than the self-attention baseline under ground-truth action histories. Consequently, neither configuration was selected for evaluation under predicted action histories.

Bidirectional Cross-Attention. While the previous modules rely on a single direction of interaction, bidirectional cross-attention (Bi-CA) allows both modalities to attend to one another. This produces a pair of cross-attended representations

$$(X'_v, X'_t) = (CA(X_v, X_t, X_t), CA(X_t, X_v, X_v)), \quad (18)$$

where $CA(Q, K, V)$ denotes cross-attention with queries Q , keys K , and values V . X'_v enriches the visual stream with

TABLE S.II: Comparison of RGB and depth feature extractors on IKEA-ASM.

Feat. Extractor	Depth	Text	Top-1/5 Acc	Recall@5
DINOv2 1B	-	-	34.37 / 83.43	43.71
DINOv3 0.8B	-	-	31.29 / 82.35	39.25
DINOv3 7B	-	-	<u>37.37 / 87.64</u>	46.57
DINOv2 1B	DAv2	-	38.82 / 86.19	46.52
DINOv3 7B	DAv2	-	38.18 / 86.95	48.75
DINOv3 7B	DA3	-	<u>39.02 / 86.87</u>	48.54
DINOv2 1B	DAv2	GT	64.51 / 94.28	62.30
DINOv3 7B	DAv2	GT	<u>65.87 / 94.20</u>	64.05
DINOv3 7B	DA3	GT	64.03 / 94.12	62.64
DINOv2 1B	DAv2	Preds	45.82 / 83.27	52.64
DINOv3 7B	DAv2	Preds	48.90 / 85.11	53.01
DINOv3 7B	DA3	Preds	48.58 / 84.55	53.22

textual cues, and X'_t injects visual information into the textual embedding.

We evaluate two projection strategies. In the *independent* variant, each direction uses its own set of projection matrices, allowing the model to learn asymmetric transformations for text-to-visual and visual-to-text attention. In contrast, the *shared* variant ties the projection weights across directions, enforcing a symmetric interaction between modalities. Although computationally lighter, the shared formulation consistently underperforms its independent counterpart, suggesting that visual and text require different attention parametrizations.

Several fusion operators are applied to combine the two attended representations, including concatenation, element-wise sum, mean fusion, embeddings product, and self-attention. Among all variants, the gated fusion achieves the strongest performance. This operator computes

$$Y = g \odot X'_v + (1 - g) \odot X'_t, \quad (19)$$

where $g \in [0, 1]$ is a learned gating vector that adaptively balances the contribution of each modality. This flexibility enables the model to downweight unreliable textual inputs under predicted action histories, leading to the best overall performance among all evaluated fusion strategies, even under the realistic setting.

B. Feature Extraction

In terms of feature extraction, we continue to use DistilBERT [54] as the text encoder due to its strong unimodal performance reported in [25]. Errors in the textual stream largely stem from the inherent ambiguity of anticipating the next action based on a short action history, rather than from limitations of the encoder itself. For this reason, our analysis focuses primarily on the RGB and depth modalities.

To assess the impact of visual feature quality, we extend the evaluation to include DINOv3 [51] (7B and 0.8B variants) and Depth Anything 3 (DA3) [52], comparing them against the original DINOv2 [49] and Depth Anything v2 (DAv2) [50].

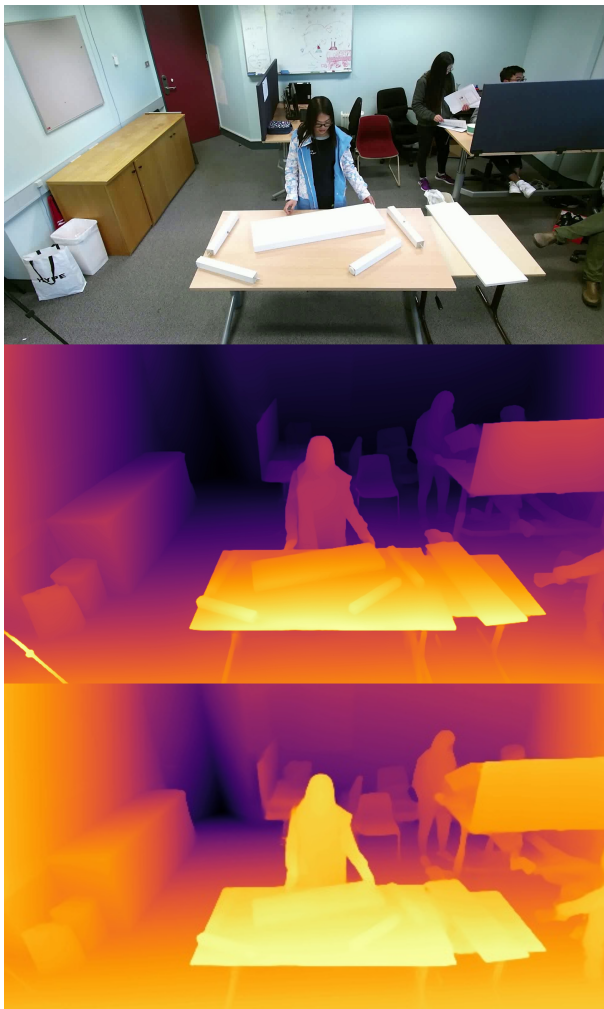


Fig. S.1: Qualitative comparison of depth frames generated by DAV2 (middle) and DA3 (bottom), with the RGB input shown on top for reference. Note how objects on the table are more clearly distinguished with DAV2 than with DA3.

Table S.II reports results across the following settings: RGB-only, RGB-Depth, RGB-Depth-Text under ground-truth action histories, and RGB-Depth-Text under predicted action histories. The latter represents the realistic operating regime of our method and constitutes the primary metric of interest.

In the RGB-only setting, DINOv3 7B consistently outperforms both the smaller 0.8B variant and DINOv2 across Top-1, Top-5, and Recall@5 metrics. This trend holds despite evaluating the 7B model in FP16 due to computational constraints, which slightly reduces numerical precision.

When introducing depth, we observe a slight decrease in performance when using DINOv3 with DAV2, whereas DA3 provides performance slightly above the DINOv2-DAV2 baseline. Despite this, when depth is combined with textual features, DAV2 yields the strongest performance under both ground-truth and predicted action histories. We attribute this to DAV2 preserving finer geometric details, as illustrated qualitatively in Figure S.1. Given its superior performance in the multimodal configuration, we adopt DINOv3 7B with Depth Anything v2 in all subsequent experiments.

TABLE S.III: Laplacian variance statistics and frame selection behavior across datasets.

Dataset	Threshold	Mean	Min	Max	Updated (%)	Too Blurry (%)
IKEA-ASM	100	301.2 \pm 125.3	128.2	801.4	0.0	0.0
Meccano	100	34.1 \pm 18.6	1.9	169.8	1.3	97.2
	50	29.2 \pm 17.2	1.9	169.8	13.1	67.9
	30	25.7 \pm 15.6	1.9	167.5	24.9	20.6
Assembly101	100	101.4 \pm 15.1	71.8	212.1	20.6	11.7

C. Blurriness Analysis

The blurriness-based keyframe selection strategy relies on a dataset-specific Laplacian variance threshold to identify visually reliable frames within a short temporal window of five frames. Since absolute Laplacian variance values depend strongly on camera motion, viewpoint, and scene structure, a single global threshold is insufficient across datasets.

Laplacian variance serves as an effective proxy for frame sharpness, with higher values indicating stronger edge responses and reduced motion blur. Empirically, values above 300 correspond to very sharp frames for which the most recent observation is already visually reliable. The range 100 – 300 represents sharp and informative frames, where multiple candidates within the temporal window often satisfy the quality criterion. Values between 50 and 100 indicate moderate blur, motivating evaluation of nearby frames, while values below 50 correspond to pronounced motion blur. Frames with Laplacian variance below 30 are severely blurred, offering limited usable structure and forcing the strategy to default to the most recent frame when no sharper alternative exists.

Table S.III reports the empirical distribution of Laplacian variance values and the resulting frame selection behavior, including the percentage of updated frames and cases where all frames within the temporal window fall below the threshold (*Too Blurry*). A threshold of 100 was chosen as default, providing robust sharpness across datasets. IKEA-ASM exhibits consistently high sharpness (mean 301.2, minimum 128.2), such that the threshold never triggers frame replacement. Meccano, in contrast, features egocentric motion and frequent blur (means 25.7-34.1), requiring additional evaluation at thresholds of 50 and 30. A threshold of 50 balances frame updates while preserving reasonable quality. Assembly101 lies in an intermediate regime (mean 101.4), where the strategy reliably identifies sharper frames within the five-frame window, yielding a large number of modified selections (20.6%) while minimizing cases where all frames are too blurry (11.7%). Frames outside these percentage ranges correspond to instances where the last frame prior to anticipation already exceeds the threshold and therefore requires no modification.

This analysis is further supported by qualitative results on the Meccano dataset, which exhibits the lowest sharpness values due to its egocentric camera setup. Figure S.2 presents qualitative examples of both selected and original frames, further demonstrating the effectiveness of the proposed method within the AAG+ framework in identifying and selecting the most informative frames.



Fig. S.2: Sample frames from the Meccano dataset illustrating motion blur caused by the egocentric head-mounted camera (left) and the corresponding frames selected by our keyframe selection method (right).

APPENDIX B

PERFORMANCE REPORT OF THE ACTION RECOGNIZER TO GENERATE ACTION HISTORY

As described in the main paper, AAG+ constructs the action history using an action recognizer with the same architecture, adapted to each recognition benchmark. All experiments are conducted using the same modalities employed for action anticipation. Baselines for comparison are dataset-specific: IKEA-ASM uses I3D [57] (Top-5 not provided), Meccano uses SlowFast [58], and Assembly101 uses TSM [59], trained on all fixed cameras. Action recognition results are reported in Table S.IV.

The proposed method outperforms the previous single-frame approach, AAG, on both IKEA-ASM and Meccano, and even surpasses some video-based methods on IKEA-ASM. On Assembly101, the model benefits from improved fusion of RGB and depth features, achieving higher performance when depth is included. However, results remain slightly below those of the original AAG and notably below video-based approaches. We attribute this gap to the increased importance of accurately modeling action history in more complex scenarios, as evidenced by the multimodal analysis of AAG+ in the anticipation setting, where longer action sequences and visually ambiguous intermediate states reduce the reliability of single-frame visual cues.

Importantly, despite lower single-frame action recognition accuracy compared to video-based methods, AAG+ achieves stronger action anticipation performance, as reported in the main paper. This improvement stems from the proposed blurriness-based keyframe selection and robustness mechanisms for handling imperfect action histories, enabling AAG+ to outperform both AAG and several video-based approaches in anticipation.

APPENDIX C COMPUTATIONAL ANALYSIS

To further highlight the computational advantages of AAG+ over existing approaches, we report a comparative analysis in Table S.V. For each state-of-the-art method considered in the main paper, we list the number of trainable parameters and the number of processed input frames. Feature extraction parameters are excluded, as feature encoders are frozen across all methods evaluated on pre-extracted features. Thus, the analysis focuses on the core model components and their input requirements.

AAG+, like its single-frame predecessor AAG, achieves competitive performance while incurring substantially lower computational overhead. Methods such as AVT and TempAgg require significantly more trainable parameters, whereas RULSTM is more compact but delivers lower performance. VLMAH is closer to AAG+ in model size, however, it relies on fine-tuned video feature extractors, which restricts training flexibility and limits adaptability across domains. In contrast, AAG+ leverages self-supervised features without task-specific fine-tuning.

Furthermore, video-based approaches process between 8 and 37 frames per sample, resulting in a proportional increase in feature extraction cost per video clip compared to AAG+'s single-frame design. While the enhanced mechanisms in AAG+ slightly increase the number of trainable parameters relative to AAG, this modest overhead yields substantial performance gains over video-based methods and enables more effective use of the available modalities.

APPENDIX D

EXTENDED MULTIMODAL ANALYSIS

In this appendix, we extend the modality contribution analysis presented in Section V to the other two modality permutations: RGB-Depth and RGB-Text, focusing on the complementary roles of RGB appearance with these contextual cues. While the main paper analyzes the interaction between visual and textual modalities, here we examine (a) the specific interaction between the single-frame RGB input and the procedural memory (textual modality), and (b) how different visual sources contribute to correct and incorrect anticipation decisions at a per-sample level.

RGB-Text Analysis. While Section V.B analyzes interactions between visual (RGB-Depth) and textual modalities, here we focus on RGB when examining visual-textual complementarity. RGB serves as the primary source of semantic and object-level information, whereas depth acts mainly as a supportive geometric cue that is most effective when (a) is fused with RGB and rarely functions as an independent predictor, and (b) under static, exocentric camera setups (see subsequent analysis). Isolating RGB therefore enables a clearer analysis of how instantaneous visual semantics interact with long-term procedural context.

The RGB-Text meta-analysis (Figure S.3) reveals a clear dataset-dependent shift in modality reliance in AAG+. On IKEA-ASM, which features shorter procedural sequences and stable third-person viewpoints, AAG+ achieves a balanced

TABLE S.IV: Single-frame action recognition performance (Top-1/5).

Methods	IKEA-ASM	Meccano	Assembly101
Video (RGB-only)	57.58 / -	45.16 / 73.75	-
Video (Multimodal)	64.25 / -	49.66 / 73.75	43.60 / -
AAG _{AR} (RGB, AH)	66.43 / 92.56	31.21 / 66.03	34.19 / 58.30
AAG _{AR} (RGB-D, AH)	66.84 / 92.29	31.14 / 66.52	32.77 / 56.19
AAG+ _{AR} (RGB, AH)	72.38 / 94.58	33.19 / 71.34	30.74 / 57.97
AAG+ _{AR} (RGB-D, AH)	72.95 / 95.04	33.79 / 73.29	31.49 / 59.09

TABLE S.V: Computational comparison.

Method	Trainable Params (M)	Processed Frames
AVT [10]	392	10
TempAgg [11]	123	37
RULSTM [12]	67	14
VLMAH [13]	45	8
AAG [25]	24	1
AAG+	34	1

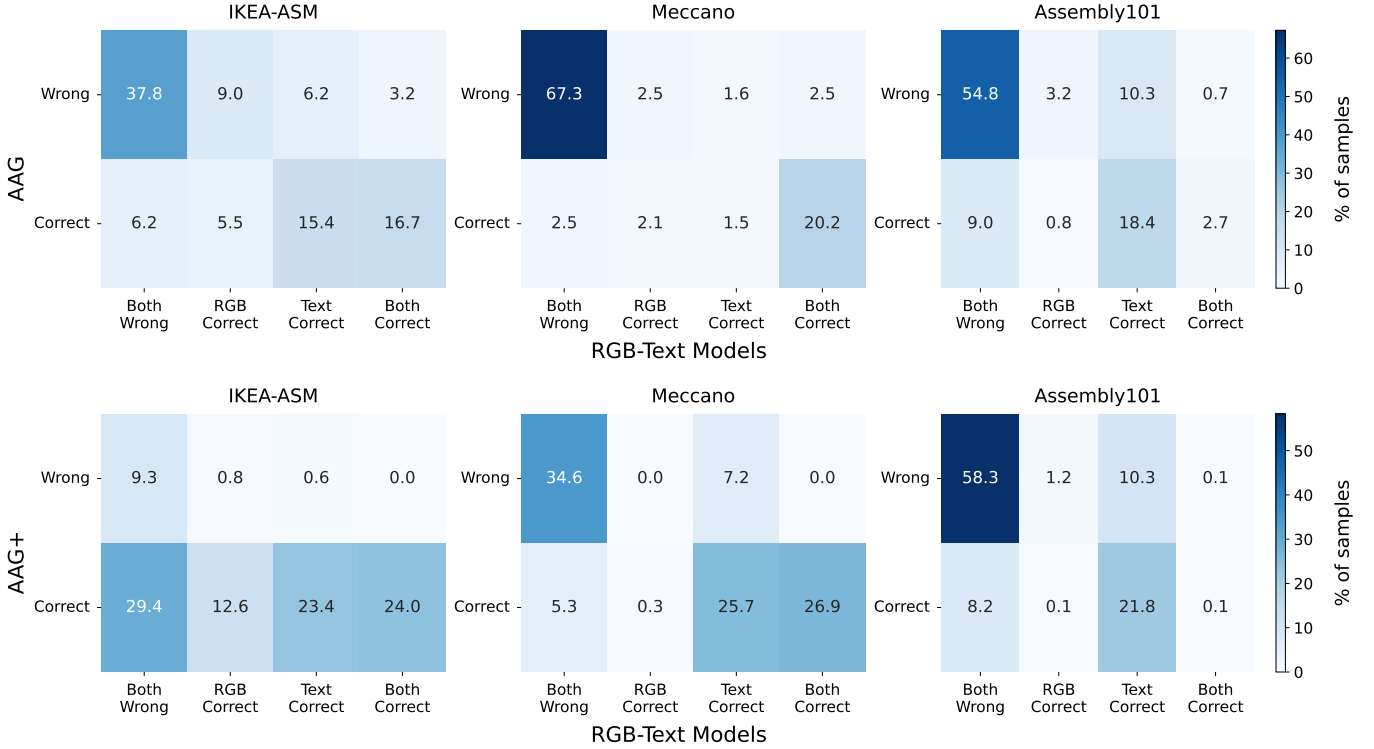


Fig. S.3: Confusion matrix-style modality breakdown for AAG and AAG+ across datasets under RGB-Text fusion.

contribution between visual and textual cues, with a substantial increase in jointly correct predictions. This indicates effective cross-modal integration, where single-frame appearance is reliably grounded by action-history semantics.

In contrast, Meccano exhibits a strong dominance of the textual modality: the vast majority of correct predictions arise from text-only or joint RGB-Text correctness, while RGB-only correctness is negligible. This reflects the fine-grained, visually repetitive nature of the task, where instantaneous visual evidence is often insufficient to disambiguate the next action without procedural context. The trend is most evident on Assembly101, where correct predictions are almost exclusively driven by the textual action-history encoder. The near absence of RGB-only and joint correctness confirms that, in long-horizon, highly variable procedural tasks, single-frame visual cues provide limited predictive power. Compared to AAG, AAG+ further consolidates this behavior, indicating that its refinements enable more decisive reliance on semantic temporal priors rather than noisy visual evidence.

Visual Analysis. An RGB-Depth meta-analysis reveals clear differences in how visual cues are exploited in AAG and

AAG+. The visual source contribution confusion-style analysis, shown in Figure S.4 reveals that the contribution of geometric cues is strongly dataset-dependent and closely tied to capture conditions and task structure.

On IKEA-ASM, which is recorded from a static third-person viewpoint with limited camera motion, depth estimates are comparatively reliable and stable. Under these conditions, AAG+ more effectively exploits geometric information than AAG, as evidenced by an increased proportion of samples in which both RGB and Depth lead to correct predictions. This shift indicates improved cross-modal alignment, where depth reinforces appearance-based cues rather than acting as a noisy auxiliary signal. In contrast, for both Meccano and Assembly101, the analysis indicates that the nature of the datasets themselves necessitates a shift away from visual dominance. In Meccano, visual modalities appear largely redundant: when the visual branch yields a correct prediction, both RGB and Depth predictors typically arrive at the decision independently. Similarly, in Assembly101, AAG+ exhibits a reduction in isolated RGB- or Depth-correct cases, relegating visual cues to a secondary role. Consequently, this verifies for both datasets,

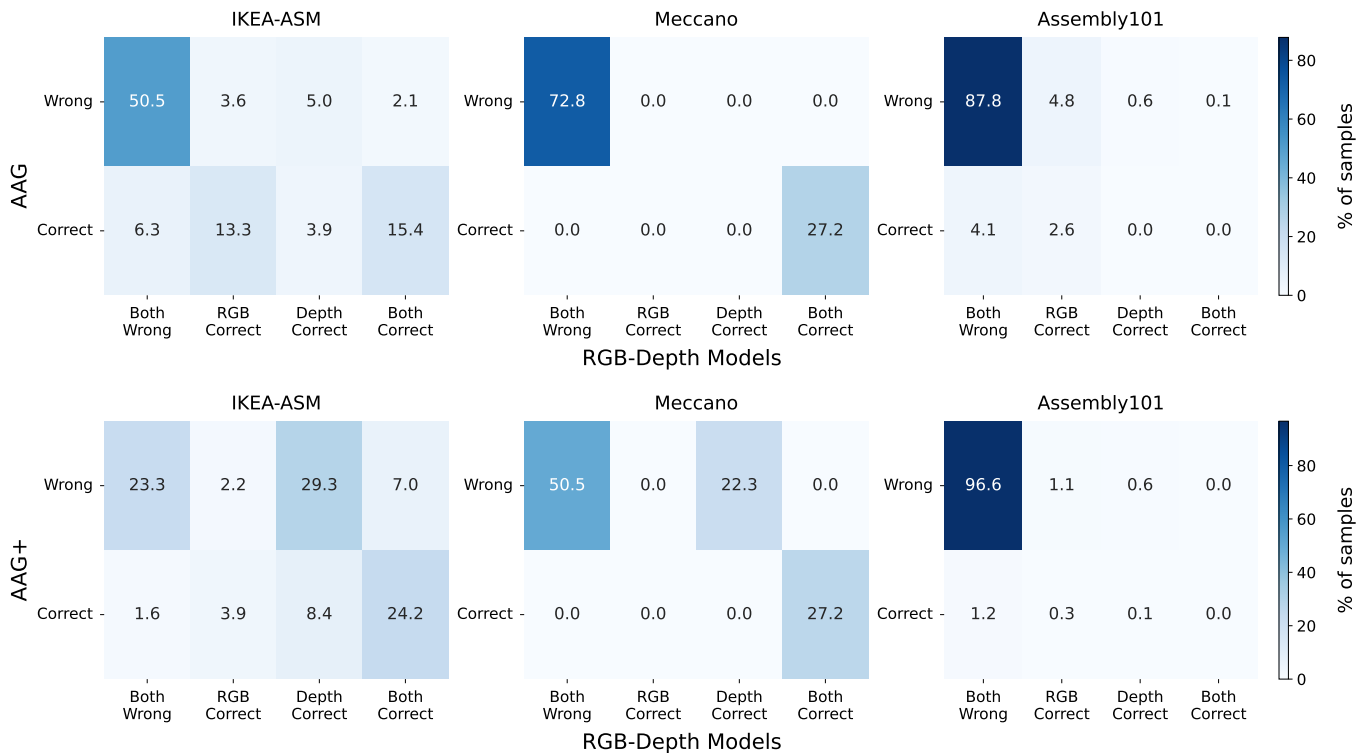


Fig. S.4: Confusion matrix-style modality breakdown for AAG and AAG+ across datasets under RGB-Depth fusion.

any significant performance increase in AAG+ is attributed to, and necessitated by, enhanced reliance on the textual modality, as the visual ambiguity and procedural complexity inherent to these domains limit the ceiling of pure visual processing.

This underscores a fundamental characteristic of procedural activity analysis: as the action space grows and action sequences become more variable, memory of past actions becomes increasingly critical for accurate anticipation. Due to the inherent visual complexity and occlusion in these scenes, specific visual information extracted from a single frame is frequently ambiguous. Thus, the model must rely on the temporal scaffold provided by the action history to disambiguate the future state.

APPENDIX E QUALITATIVE COMPARISON OF VLMS FOR ACTION HISTORY RETRIEVAL

We conduct a qualitative evaluation of VLMS to gain deeper insights into their behavior across different prompt formulations, task complexities, and viewpoints. Figure S.5 illustrates the two prompt variants used in the main paper, short and long fine-grained prompts, designed to assess the impact of instruction granularity. We then report results for each dataset on frames where the single-frame action recognizer performs well. For each example, we present: (1) the current action, (2) the previous five actions, and (3) the model’s rationale for predicting these actions. To facilitate analysis, correct observations are highlighted in green, incorrect ones in red, and model assumptions are shown in yellow.

We should note that we additionally experimented with Llama-4 Maverick under the same prompt formulations. However, its outputs were consistently less coherent and substantially less aligned with the ground-truth action histories than both GPT 5.1 and Gemini 3 Flash. For this reason, we omit qualitative examples for Llama-4 Maverick.

The behavior observed on the IKEA-ASM dataset, shown in Figure S.6, is consistent with the quantitative evaluation. Gemini 3 Flash generally outperforms GPT-5.1, which, under fine-grained prompts, often fails to correctly identify the ongoing action and consequently mispredicts past actions. We further observe that the VLMS sometimes rely on prior knowledge or assumptions rather than visual evidence of the current state and objects. VLMS still lack precise moment-level information, highlighting both the effectiveness of the action recognizer for this task and the limitations of current language-based models for this task.

Figure S.7 presents the qualitative results on the Meccano dataset. In contrast to the previous dataset, partial observation of an action in this setting negatively affects VLM behavior: when only the final frames of the *take_bolt* action are visible, the visual evidence leads the vision-language models to predict *plug_screw* instead. This example further highlights the limitations of these models, which, despite being significantly heavier than the action recognizer, fail to match its performance. Notably, the explicit action history leveraged by the action recognizer, or the temporal modeling employed by video-based methods, helps disambiguate such cases and enforces the logical ordering of actions: a bolt cannot be plugged unless it has first been taken.

You are an expert in assembly actions. Analyze the attached image.
Available actions: [dataset dependent list]

Task:

1. Identify the current action (from the list above).
2. Infer the 5 most plausible previous actions (earliest → most recent) that led to this state.
3. Show me the rationale behind your answer, written in a single paragraph.

Output format:

Current: [action class]

Previous: [action1, action2, action3, action4, action5]

(a) Short fine-grained prompt.

You are an expert in recognizing fine-grained human assembly actions from a single frame.

Observation: [Attached image]

Available action classes (use only these when naming actions): [dataset dependent list]

Follow these steps carefully:

ASK:

1. Identify the ****current action**** being performed in this frame.
2. Examine key visual cues: hand/object interaction, object placement or orientation, body posture, and assembly context.
3. Give me the rationale behind your answers in a single paragraph.

HINT:

3. Consider what ****previous actions logically led to this configuration****.
 - Infer object placement, preparation steps, and assembly progression from the visual state.

TEMPORAL RECONSTRUCTION:

4. Using only the available action classes, reconstruct the ****five most plausible previous actions**** (earliest → most recent) that directly led to the current action.
5. Show me the rationale behind your answers in a single paragraph.

OUTPUT FORMAT (strictly follow this):

Current Action: [one action class from the list]

Previous Actions (earliest → most recent):

(b) Long fine-grained prompt.

Fig. S.5: Fine-grained prompts for action history retrieval. (a) Short version, which concisely summarizes past actions for efficient retrieval. (b) Long version, which includes richer contextual details to support more accurate retrieval. When action sequences are available, they are provided as an attached file, and the model is explicitly informed of its existence.

Finally, qualitative results on the Assembly101 dataset are presented in Figure S.8. This dataset includes both assembly and disassembly processes, which pose a significant challenge for VLMs. Notably, Gemini produces more coherent results than GPT, which often relies on erroneous visual observations. However, even when Gemini correctly interprets the current observation, assumptions about an assembly (rather than a disassembly) process lead to completely incorrect predictions for previous actions.



GT past actions: pick up leg; spin leg; NA; pick up leg; NA; spin leg; tighten leg

Gemini 3 Flash - Short Prompt

Current Action: spin leg

Previous Actions: pick up table top, lay down table top, lay down leg, pick up leg, align leg screw with table thread

Rationale: The user is currently kneeling on the floor and holding a table leg perpendicular to the corner of the large table top. His hand grip around the leg shaft suggests a rotating motion used to thread the leg into the table's mounting plate, which corresponds to the action spin leg. Before reaching this specific point in the assembly, the user logically must have prepared the workspace by bringing the main board into position (pick up table top and lay down table top) and staging the components nearby, as evidenced by the other legs on the floor (lay down leg). Following the setup, the immediate preceding steps would involve retrieving the specific leg currently being installed (pick up leg) and positioning its screw directly over the hole (align leg screw with table thread) before beginning to spin it.

GPT 5.1 - Short Prompt

Current Action: pick up side panel

Previous Actions: pick up leg, lay down leg, lay down bottom panel, lay down side panel, lay down back panel

Rationale: The person is kneeling and holding a vertical board, grasping it with both hands in a way consistent with picking up a side panel prior to aligning or attaching it. Several flat boards (likely bottom, back, and another side panel) are already placed on the floor, indicating that earlier steps involved laying these panels down and positioning legs. The scattered components and the partially assembled configuration suggest the user has moved sequentially from placing structural parts on the ground to picking up the next side panel to continue assembly

Gemini 3 Flash

Current Action: spin leg

Previous Actions: pick up table top, lay down table top, lay down leg, pick up leg, align leg screw with table thread

Rationale: The man is currently executing the action spin leg as he kneels and rotates the black leg to secure it into the upside-down table top, a step confirmed by his grip on the leg shaft and the distinct upright orientation of the leg against the board. This action is the culmination of a clear linear sequence where the assembler first prepared the workspace by bringing the board in (pick up table top) and placing it inverted on the floor (lay down table top) to access the mounting points. Following this setup, he likely organized the loose parts (lay down leg), then selected the specific leg (pick up leg) and positioned it precisely over the corner hole (align leg screw with table thread) to enable the current threading motion.

GPT 5.1

Current Action: tighten leg

Previous Actions: lay down table top, pick up leg, lay down leg, align leg screw with table thread, spin leg

Rationale: The rationale for identifying the current action as tighten leg: The person is kneeling close to the underside of a table component and applying force with both hands to a vertical leg element that is already attached to the tabletop. The posture, proximity, and focused hand-leg interaction indicate a final fastening step rather than alignment or pickup. The leg is upright and engaged with the tabletop, implying the screw thread has already been engaged and is now being tightened to secure the leg firmly, which logically follows earlier alignment and spinning actions. The rationale for the previous actions: The tabletop must first be laid down to expose its underside for assembly. A leg is then picked up and positioned (laid down/upright) near the attachment point. Before tightening, the leg screw needs to be aligned with the table's threaded insert, after which the leg is spun by hand to engage the thread. These steps naturally culminate in the current action of tightening the leg to complete the attachment.

Fig. S.6: VLMs qualitative results on IKEA-ASM dataset. Note the colors noting correct observations (green), incorrect (red) or assumed (yellow).



Ground Truth

Current Action: take_bolt

Past Actions: check_booklet;
check_booklet; align_objects; plug_screw;
check_booklet

Gemini 3 Flash - Short Prompt

Current Action: plug_screw

Previous Actions: check_booklet, take_screw, take_gray_angled_perforated_bar, take_gray_perforated_bar, browse_booklet

Rationale: The image shows a person assembling a model using various parts, with their hands holding a gray angled perforated bar and a red screw. The presence of an instruction booklet and the specific parts being used suggests that the person is following a set of instructions to assemble the model. **The current action of plugging the screw into the bar is a natural step in the assembly process.** The most plausible previous actions would have involved preparing for this step by checking or browsing the booklet to understand the instructions, and taking the necessary parts such as the gray angled perforated bar, gray perforated bar, and red screw.

GPT 5.1 - Short Prompt

Current Action: screw_screw_with_hands

Previous Actions: take_gray_perforated_bar, take_red_perforated_bar, align_objects, take_screw, put_screw

Rationale: In the image, the hands are holding two perforated bars (a gray one and a red one) already aligned, while **the right hand is rotating a red screw using fingers.** This indicates the assembly step of manually fastening the screw, corresponding to screw_screw_with_hands. To reach this moment, the user would have picked up the gray bar, then the red bar, aligned their holes, taken a screw, inserted it (put_screw), and is now tightening it by hand.

Gemini 3 Flash - Long Prompt

Current Action: plug screw

Previous Actions: browse booklet, take gray perforated bar, take white angled perforated bar, align objects, take screw

Rationale: The person is currently performing the action plug screw, as **they are seen physically inserting a red fastener into the pre-aligned holes of two structural bars.** This specific action follows a logical progression where the builder first consulted the manual (browse booklet) to identify the assembly step, then retrieved the necessary structural components (take gray perforated bar and take white angled perforated bar). Once the parts were in hand, they were brought together to match their respective holes (align objects), and finally, the builder reached for the connector (take screw) to begin the current insertion process.

GPT 5.1 - Long Prompt

Current Action: plug screw

Previous Actions: take gray perforated bar, take red perforated junction bar, take screw, align objects, put screw

Rationale: In the image, both hands are holding two perforated bars (a gray angled bar and a gray straight bar) while a red screw is being manually inserted through aligned holes, without any screwdriver or wrench in use. **The fingers are pushing the red fastener straight through the perforations, indicating an insertion/plugging motion rather than tightening, aligning a tool, or screwing.** The assembly context (instruction booklet open to the relevant step, parts already oriented and overlapping) implies that the bars were previously picked up, brought together, and aligned, after which a screw was selected and placed at the joint. This configuration naturally leads to the current action of plugging the screw by hand to temporarily fix the parts before any tightening step.

Fig. S.7: VLMs qualitative results on Meccano dataset. Note the colors noting correct observations (green), incorrect (red) or assumed (yellow).



Ground Truth

Current Action: put down arm connector
Past Actions: unscrew arm connector with screwdriver; rotate partial toy; remove roller arm; put down partial toy; remove arm connector

Gemini 3 Flash - Short Prompt

Current Action: pick up screwdriver

Previous Actions: pick up cabin, position cabin, pick up screw, position screw on cabin, screw cabin with screwdriver

Rationale: The image shows a person reaching for a small red-handled tool (a screwdriver) while toy components are scattered on the workspace, including a detached cabin and a chassis. The user's left hand is already holding an orange component (likely the dump bed or body), while the right hand moves to pick up the screwdriver to begin or continue an assembly step. Based on the presence of the cabin near the chassis, it is highly plausible that the previous actions involved retrieving the cabin, positioning it onto the main toy body, and preparing to secure it by positioning a screw. The chronological sequence suggests a transition from manual positioning of parts to the tool-use phase required for fastening components together.

GPT 5.1 - Short Prompt

Current Action: position screw on cabin

Previous Actions: pick up cabin, position cabin, pick up screw, pick up screwdriver, pass screw to other hand

Rationale: In the image, the person is holding a red-handled screwdriver in one hand while guiding a screw toward a yellow cabin-shaped toy part held steady on the table, which matches the action of position screw on cabin from the provided action list. The cabin component is already separated and oriented upright, implying it was previously picked up and positioned. Before positioning the screw, the screw itself must have been picked up, and the screwdriver acquired to enable fastening. The hand posture suggests the screw may have been transferred between hands for alignment, making pass screw to other hand a plausible immediate precursor. These actions align with typical assembly sequences defined in the action list.

Gemini 3 Flash - Long Prompt

Current Action: position screw on cabin

Previous Actions: pick up cabin, position cabin, pick up screw driver, screw cabin with screwdriver, pick up screw

Rationale: The person is currently holding a small red-capped object, which serves as a screw container or the screw itself, and is placing it onto the yellow cabin component situated on the workspace. This is a preparatory step for securing the cabin to the chassis. Before this, the assembly sequence logically required picking up the cabin and positioning it on the vehicle body. The presence of a screwdriver and previous "screw" actions in the log suggest that the cabin was already partially worked on or is being prepared for final fastening. The visual state shows the cabin resting on the table near the main chassis, indicating that the immediate progression involves adding fasteners to the specific sub-assembly currently being manipulated by the left hand.

GPT 5.1 - Long Prompt

Current Action: push partial toy

Previous Actions: pick up partial toy, rotate partial toy, put down partial toy, pick up cabin, position cabin

Rationale: In the frame, one hand is holding a red applicator bottle and applying pressure to dispense material directly onto a small yellow toy subcomponent resting on the table, while the other hand stabilizes another toy part. There is clear hand-object interaction with a stationary, partially assembled toy element, and the applied force indicates an active manipulation rather than placement or pickup. Since no screwdriver or screw is involved and the action involves applying pressure to the toy assembly itself, the closest matching atomic class is push partial toy. The preceding actions logically involve picking up and rotating a partial toy to orient it correctly, putting it down on the workspace, and positioning a cabin component nearby, which sets up the configuration where adhesive or pressure is applied to advance the assembly process.

Fig. S.8: VLMs qualitative results on Assembly101 dataset. Note the colors noting correct observations (green), incorrect (red) or assumed (yellow).